PERGAMON

Atmospheric Environment 35 (2001) 6049–6072

ATMOSPHERIC ENVIRONMENT

www.elsevier.com/locate/atmosenv

The effect of water on gas–particle partitioning of secondary organic aerosol. Part I: α-pinene/ozone system

David R. Cocker III[a], Simon L. Clegg[b], Richard C. Flagan[a], John H. Seinfeld[a,]*

[a] *Department of Environmental Engineering Science and Department of Chemical Engineering, California Institute of Technology, Pasadena, CA 91125, USA.*

[b] *School of Environmental Sciences, University of East Anglia, Norwich NR4 7TJ, UK*

Received 10 February 2001; accepted 29 July 2001

Abstract

The effect of relative humidity (RH) on aerosol formation by the semi-volatile oxidation products of the α-pinene/O_3 system has been comprehensively studied. Experiments were performed in the presence of ammonium sulfate (aqueous, dry), ammonium bisulfate seed (aqueous, dry), and aqueous calcium chloride seed aerosols to ascertain their effect on the partitioning of the oxidation products. The yield of organic aerosol varies little with RH, and is not affected by the presence of dry inorganic salt aerosols. Aqueous salt aerosols reduce the yield of organic aerosol compared to that under seed-free or dry seed conditions. The degree of reduction is electrolyte dependent, with aqueous ammonium sulfate leading to the largest reduction and aqueous calcium chloride the smallest. Hygroscopic growth of the organic aerosol from $<2\%$ to 85% RH was also monitored, and could be satisfactorily represented as the sum of the individual contributions of the organic and inorganic fractions. The implications of the growth factor measurements for concentration/activity relationships of the condensed phase organic material (assuming a liquid solution) was explored. The formation of the organic aerosol was investigated using a simple two component model, and also one including the 12 product compounds identified in a previous study. The experimental results for $<2\%$ and 50% RH (without salt seed aerosols) could be satisfactorily predicted. However, the aqueous salt seed aerosols are predicted to increase the overall yield due to the dissolution of the organic compounds into the water associated with the seed aerosol— the opposite effect to that observed. The implications of two distinct phases existing the aerosol phase were investigated.

Keywords: Secondary organic aerosols; Relative humidity; Biogenic hydrocarbons

1. Introduction

Atmospheric oxidation of organic molecules containing roughly six or more carbon atoms can lead to products of sufficiently low vapor pressure that they partition between the gas and aerosol phases. The aerosol fraction of these products is known as secondary organic aerosol (SOA). Over the last decade, there have been a number of laboratory studies of the SOA-forming potential of both anthropogenic and biogenic organics (Griffin et al., 1999; Hoffmann et al., 1997; Odum et al., 1996, 1997; Edney et al., 2000). This work has demonstrated convincingly that the mechanism of SOA formation is absorptive partitioning of the oxidation products between the gas-phase and a particulate organic absorbing phase. With few exceptions, laboratory and smog chamber studies on SOA formation have been carried out at relative humidities (RH) sufficiently close to zero that the resulting aerosol is water-free. Experiments conducted under dry conditions are an essential first step in understanding the partitioning of organic products to the aerosol phase. Dry inorganic seed aerosol has frequently been used as an inert surface

---

*Corresponding author. Fax: +1-818-585-1729.
E-mail address: seinfeld@caltech.edu (J.H. Seinfeld).

1352-2310/01/$ - see front matter © 2001 Elsevier Science Ltd. All rights reserved.
PII: S1352-2310(01)00404-6

upon which SOA forms and grows. In experiments carried out under dry conditions in both the presence and absence of seed aerosol, it has been found that the ultimate amount of aerosol formed is the same in both cases (Odum et al., 1996).

Ambient RHs are frequently such that atmospheric aerosols contain water. Understanding the water associated with inorganic atmospheric aerosols has occupied considerable attention in the literature over the past two decades (Pilinis and Seinfeld, 1987; Wexler and Seinfeld, 1990, 1991; Kim et al., 1993a, b; Kim and Seinfeld, 1995; Jacobson et al., 1996; Clegg et al., 1992, 1998a, b; Nenes et al., 1998; Zhang et al., 2000) suffice it to say that prediction of the liquid water content of inorganic aerosols can now be made with considerable confidence. Atmospheric particles are, by and large, a mixture of both inorganic and organic components. Due to the wide variety of atmospheric organic compounds, the complex nature of organic–water molecular interactions, and the paucity of thermodynamic data on organic/water systems of atmospheric relevance, predicting the water associated with organic components of atmospheric aerosols is not yet possible on a general scale.

Water is likely to play a role in gas–particle partitioning of low vapor pressure oxidation products, potentially affecting the thermodynamic equilibrium achieved between gas- and aerosol- phase organics. Absorption of water into the organic phase of the aerosol may alter the activity of the organic constituents in solution, thus perturbing the fraction of organic material present at equilibrium in the aerosol from that in the absence of water. Inorganic particles, at sufficiently high RH, can deliquesce, transforming the aerosol from a dry salt to an aqueous solution of high electrolyte concentration. The appearance of electrolytes could, in turn, alter the organic gas–particle thermodynamic equilibrium by changing the activity of the absorbing organic phase, especially if the water–electrolyte–organic mixture exists as a single phase in the aerosol. The goal of this work is to study experimentally how the yield of SOA is affected by the presence of liquid water in the aerosol phase. Upon atmospheric oxidation, each parent hydrocarbon yields its own characteristic set of oxidation products. As a result, it is likely that the presence of liquid water will not affect all SOA in the same manner. An appropriate system to begin a comprehensive study of the effect of RH on SOA formation is one that has been well-studied in the dry state and one for which, if possible, the molecular composition of the aerosol has been identified. The α-pinene/O_3 system satisfies these conditions. We consider the relatively well-studied α-pinene/O_3 system (Hoffmann et al., 1997; Virkkula et al., 1999; Yu et al., 1999; Griffin et al., 1999) as a benchmark to study how the yield of SOA is affected by the presence of liquid water in the aerosol phase and the role of the inorganic seed aerosol in gas–particle partitioning.

We begin with a description of the experimental apparatus and procedures used to generate and measure α-pinene/O_3 SOA in the presence and absence of inorganic seed and water. Next, we discuss the experimental investigation of the role of water and the inorganic seed in aerosol formation and hygroscopic behavior. We then attempt to explain the experimental results obtained on theoretical grounds.

2. Experimental description

Experiments were performed in an indoor, dual 28 m^3 Teflon reactor. In this configuration, two experiments could be performed simultaneously under identical temperature conditions. Temperature and RH in the system could be controlled from 20°C to 50°C at a precision of ± 0.5°C and 1–85% at a precision of $\pm 0.5\%$, respectively. Particle-phase instruments, and their sampling lines, were maintained at the identical temperature of the reactor.

Hydrocarbon measurements were carried out using a Hewlett-Packard (Palo Alto, CA) 5890 Series II Plus gas chromatograph (GC) utilizing a DB-5 60 m column (J&W Scientific, Davis, CA) and a flame ionization detector (FID). The GC temperature program was as follows: -50°C for 1 min, -50 to –150°C at 40°C min^{-1}, held at 150°C for 1 min. Estimated uncertainty of the hydrocarbon measurement is 2%.

Aerosol size distributions and number concentrations were obtained every 60s using two cylindrical (TSI model 3071) scanning electrical mobility spectrometers (SEMS), one for each chamber. Each SEMS was equipped with a TSI model 3760 condensation particle counter (CPC). Sheath and excess flow was set to 2.5 l min^{-1} with the inlet and classified aerosol flow of 0.25 l min^{-1}. Voltages were ramped from 30 to 7000 V, allowing for measurement of 25–700 nm diameter particles. Volumetric flow control to within $\pm 0.5\%$ was achieved by measuring the pressure drop of the gas flow across a laminar flow element and adjusting the flows with proportional control valves (MKS model 248A). These valves were then interfaced to Labview software (National Instruments, Houston, Texas) using proportional–integral–differential (PID) control that can update the flow at a rate of 100 s^{-1}. The data inversion routine accounts for charging and counting efficiency as well as particle loss (Collins et al., 2001). Additional TSI 3010 CPCs were used to monitor the total number concentration in the chamber and for correction of SEMS generated number concentrations.

A tandem differential mobility analyzer (TDMA) was used to determine the hygroscopic uptake of water by the aerosol produced in the chamber. The TDMA follows the initial design of Rader and McMurry (1986) and includes the volumetric flow control of the SEMS mentioned above. The residence time of the TDMA humidification chamber is 10 s, and the RH can be varied from 5% to 89% with approximately 0.5% accuracy. Hygroscopic growth data were obtained for chamber aerosol with initial classified diameters of 136 and 235 nm.

The SEMS were calibrated at multiple diameters using polystyrene latex spheres (Duke Scientific, Palo Alto, CA) with a resolution of ±3%. The two SEMS were then calibrated against each other in a tandem arrangement to ensure proper measurement. TDMA calibration was performed by fixing the voltage of the first DMA column and measuring the diameter of dry $(NH_4)_2SO_4$ particles in the second column without altering the gas-phase composition, RH, or temperature surrounding the particles. Furthermore, the TDMA G_f were compared to other measured and modeled values and were found to be quite accurate. (For details, see Section 5.4.) Based on these measurements, the estimated accuracy for particle electrical mobility from the Caltech SEMS and TDMA is ±0.3%. The accuracy of the hygroscopic growth factors using the TDMA is limited to the control of RH to ±0.5% in the humidification chamber; the true accuracy will be a function of the particles response to RH fluctuations which is largely dependent upon the RH and composition of the aerosol. More operational, sensitivity, and accuracy information is reported in Cocker et al. (2001a).

Prior to each experiment, the chambers were flushed with purified compressed laboratory air. The laboratory compressed air was processed via four packed bed scrubbers containing activated carbon, silica gel, Purafil, and 13 × mol sieve, respectively, followed by a filter. The resulting air had no detectable reactive organic gases or particles, and <2 ppb NO_x.

Controlling the RH of the Teflon chambers was achieved using a 1500 W immersion heater submersed into a 60 cm tall, 7.5 cm diameter glass cylinder fitted with a Teflon cap. Triple deionized water with a minimum conductivity of $18.2\,M\Omega^{-1}$ was added to the glass cylinder. The steam generated was passed through 2.5 cm diameter Teflon tubing into the chamber, allowing for a RH of 50% to be achieved in approximately 40 min. RH and temperature were measured using a Vaisala (HMP233) capacitance meter with stated temperature accuracy of ±0.1% and RH accuracy of ±0.5%. The process of adding gas-phase water did not introduce any detectable aerosol or organics into the chambers.

After allowing the humidity of the chamber to stabilize, initial seed aerosol was generated from 0.005 M solution of either $(NH_4)_2SO_4$, NH_4HSO_4, or $CaCl_2$, using a stainless steel, constant rate atomizer to a number concentration of about $2\times10^4\,cm^{-3}$ of 80 nm mean diameter particles for a total aerosol volume of 2–10 $\mu g\,m^{-3}$. Moist seed aerosol was generated by directly passing the aerosol to a previously humidified chamber; dry seed aerosol was generated by passing the atomized solution through a heated line and then a Nafion diffusion dryer with exiting RH <15%. In both cases, the aerosol stream was passed through ^{210}Po charge neutralizers before entering the chamber.

For the dark ozonolysis experiments, 2-butanol, which was used as a hydroxyl radical scavenger, and α-pinene were introduced at least 1.5 h before starting the experiment. 2-Butanol was injected at sufficient concentrations (680 times, by volume, of α-pinene injected) that the reaction rate of OH radicals (generated in the α-pinene/O_3 reaction) with butanol exceeded that with α-pinene by a factor of 100. NO_x levels were kept below 2 ppb. Initial measurements of the α-pinene, 2-butanol, and ozone were made prior to the start of the experiment. A minimum of three initial hydrocarbon measurements were taken for each chamber, and subsequently repeated every 11 min. Experiments commenced by injecting ozone into the reactor at a mixing ratio of approximately 30 ppm at a rate of $5\,l\,min^{-1}$ for about 1 h. Ozone was monitored with a Dasibi Environmental Corp. (Glendale, CA) Model 1008-PC O_3 analyzer. Ozone measurements were taken in 10 min intervals for both chambers and have estimated uncertainties of ±4%. Temperature and RH were monitored over the course of the reaction. The reader is referred to Cocker et al. (2001) for further description of the environmental chamber, instrumentation used (including precision and accuracy), and the procedures followed at the facility.

3. Aerosol yield

Due to the difficulty associated with the molecular identification and quantification of secondary organic compounds derived from the oxidation of parent hydrocarbons, the aerosol yield has been used as a measure of the overall aerosol forming potential of various hydrocarbons (Griffin et al., 1999). Aerosol yield, Y, is defined as the ratio of ΔM ($\mu g\,m^{-3}$), the aerosol mass concentration produced through oxidation of the parent hydrocarbon, to ΔHC ($\mu g\,m^{-3}$), the mass concentration of parent gas-phase organic reacted, $Y = \Delta M/\Delta HC$.

An absorptive partitioning model proposed by Pankow (1994a, b) has been demonstrated extensively (Odum et al., 1996, Griffin et al., 1999) to describe SOA formation. Gas-phase organic compounds partition into the aerosol phase below supersaturation through absorptive dissolution into the organic phase present. Once a threshold amount of secondary organic material is present to form an initial organic layer, gas–particle partitioning ensues. The aerosol yield Y resulting from the oxidation of a single parent hydrocarbon can be described as the sum of the yields of each organic product Y_i as follows:

$$Y = \sum_i Y_i = \Delta M_{\mathrm{org}} \sum_i \frac{\alpha_i \mathrm{K}_{\mathrm{om},\,i}}{1 + \mathrm{K}_{\mathrm{om},\,i} \Delta M_{\mathrm{org}}}, \tag{1}$$

where α_i is the mass-based stoichiometric fraction of species i formed from the parent hydrocarbon, $K_{\mathrm{om},\,i}$ is the gas–particle partitioning coefficient ($\mathrm{m}^3\,\mu\mathrm{g}^{-1}$), which is inversely proportional to the compound's vapor pressure, and ΔM_{org} ($\mu\mathrm{g\,m}^{-3}$) is the total mass concentration of organic material and associated water present in the aerosol phase. The fraction of secondary organic material condensing into the aerosol phase is seen to depend on the amount of organic aerosol mass present. Although numerous products are formed in the oxidation of a single parent hydrocarbon (Yu et al., 1999; Forstner et al., 1997), it has been shown that an empirical two-product model accurately represents yield data obtained for more than 30 parent hydrocarbons (Odum et al., 1996; Hoffmann et al., 1997; Griffin et al., 1999). Essentially, one product represents the more volatile compounds while the other describes the products of lower volatility (Odum et al., 1996).

4. Experimental protocol

Our goal is to gain a fundamental understanding of two phenomena: (1) the effect of water on the yield of SOA; and (2) the effect of the presence and nature of an inorganic electrolyte salt on the yield of SOA. Both phenomena are prevalent in the ambient atmosphere. Our approach is to address these issues both experimentally and theoretically. This section outlines the experimental protocol employed to isolate each of the phenomena. Five classes of experiments were conducted: SOA formation in the absence of a seed aerosol under dry and humid conditions; SOA formation in the presence of a dry seed aerosol under dry and humid conditions; and SOA formation in the presence of a wet (inorganic electrolyte) seed aerosol under humid conditions.

4.1. Dry nucleation

SOA produced under dry conditions with no seed aerosol is 100% organic in content. Initial particle formation results from a sufficient supersaturation of low volatility organics to produce homogeneous nucleation followed by condensation to the aerosol. The organic aerosol produced is simply the final measured volume of the aerosol, after correcting for wall loss. The aerosol mass concentration is estimated from the aerosol volume by assuming a density of $1\,\mathrm{g\,cm}^{-3}$, consistent with the density and mixture of organic products of α-pinene/O_3 oxidation as reported by Yu et al. (1999). The yield curve (Y as a function of ΔM_{org}) generated from such an experiment provides a pure "baseline" of the system—the amount of SOA formed in the absence of either inorganic constituents or water.

4.2. Humid nucleation

The SOA produced in the absence of seed aerosol but at elevated RH values, so-called humid nucleation experiments, consists of organic compounds and liquid water. As in the dry, seed-free case, the initial aerosol is produced by nucleation of supersaturated oxidation products; however, the subsequent growth of the aerosol results from absorption of both organics and water (if the organic products are sufficiently hydrophilic). The total aerosol formed, in this case, will depend on organic–organic and organic–water interactions. The mass concentration of organic aerosol produced is the total aerosol mass concentration less the mass concentration of water associated with the aerosol. The water content of the aerosol cannot be directly measured but may be inferred experimentally as follows. Aerosol produced under dry nucleation conditions contains no water. The tandem differential mobility analyzer (TDMA) is used to measure the change in particle diameter that occurs when the RH surrounding this pure organic aerosol is raised to RH conditions corresponding to the humid experiments. The water content of the wet aerosol is estimated from the dry and wet diameters measured in the TDMA as

$$M_{\mathrm{water}} = M_{\mathrm{total}}(D_{p,\,\mathrm{d}}/D_{p,\,\mathrm{w}})^3. \tag{2}$$

4.3. Dry seed, dry conditions

In the experimental protocol most frequently followed in SOA formation studies, dry inorganic aerosol (inert, non-volatile, crystalline) is injected into the chamber to provide a surface upon which semi-volatile organic compounds condense. SOA initially forms via condensation onto the inorganic particles; subsequent growth occurs via absorption into the organic surface coating the inorganic core. The resulting aerosol composition is a mixture of organic and inorganic constituents, although in most experiments the amount of SOA ultimately deposited on the dry inorganic seed greatly exceeds the mass of initial seed, so the SOA yield is effectively equal to the final mass of the aerosol in the chamber, after wall losses have been accounted for. We will see that the inorganic seed aerosol does not affect the final yield attained; it acts simply as a substrate for aerosol condensation.

4.4. *Dry seed, elevated RH*

Dry inorganic seed particles provide an inert crystalline surface upon which condensation of organic vapors occurs. Under humid conditions, but at an RH below the deliquescence point of the seed aerosol, condensed organic vapors create an organic layer for further gas-phase absorption of both organic compounds and water. We note that Cruz and Pandis (2000) determined the deliquescence point of several salts with and without organic coatings and found no measurable difference in the presence of organic material. Thus, unless the condensable organic compounds in the present experiments are associated with significant amounts of liquid water, it is likely that the salt seed remains mostly solid and gas–aerosol partitioning is governed by organic–organic and organic–water interactions in the condensed phase. The volume concentration of SOA produced ($\mu m^3\,m^{-3}$), including any water taken up, is given by

$$V_{\text{org+water}} = V_{\text{total}} + V_{\text{wall correction}} - V_{\text{salt}}. \tag{3}$$

The amount of water is estimated from TDMA measurements as follows. Aerosol generated in the dry seed experiments at zero RH is humidified up to 50% to determine the amount of water associated with the organic at 50% RH using Eq. (2). None of the water is associated with the seed since the RH is below the RH of deliquescence. The mass $\Delta M_{\text{org+water}}$ is equated to volume, as we assume unit densities of both the SOA and its mixtures with water.

4.5. *Aqueous seed, elevated RH*

For this system, the RH of the chamber is raised prior to injection of seed aerosol. Seed aerosol, produced via a constant flow atomizer, is introduced to the chamber above its efflorescence point, resulting in an initial aqueous-phase electrolyte aerosol. Semi-volatile organic oxidation products generated by the reaction partition to the aqueous salt aerosol by condensation. The volume concentration of organic material present in the aerosol, including the change in water content in the aerosol, is given by

$$V_{\text{org+water}} = V_{\text{total}} + V_{\text{wall correction}} - V_{\text{salt+water}}. \tag{4}$$

In the above equation $V_{\text{salt+water}}$ is the initial volume of aqueous salt seed aerosol, for which the water content can be calculated using an inorganic thermodynamic model. The volume $V_{\text{org+water}}$, therefore, includes not only the amount of water taken up by the aerosol by the organic material but also any change in the total water content due to activity effects of the mixed organic/salt solution. Unit density of the volume element $V_{\text{org+water}}$ is again assumed when converting to mass, $\Delta M_{\text{org+water}}$.

5. Effect of RH on SOA formation in the α-pinene/ozone system

Forty-seven experiments were performed measuring the SOA yield of α-pinene in the dark reaction with ozone in the presence of 2-butanol as a hydroxyl radical scavenger. These experiments included ones in which no seed particles were initially present (where aerosol is formed by homogeneous nucleation), with ammonium sulfate present as either a dry inorganic seed or an aqueous inorganic seed, with ammonium bisulfate present as either a dry inorganic seed or an aqueous inorganic seed, and with calcium chloride as an aqueous inorganic seed. All experiments were performed at temperatures near 301 K. Table 1 summarizes the conditions for each of these experiments, including initial α-pinene and ozone concentrations, aerosol yields, RH, and temperature. Fig. 1 summarizes yield versus total aerosol mass concentration for all 47 α-pinene/O_3 experiments. Note that the yield includes both organic and water contributions for experiments carried out under humid conditions.

The data have been fit to a two-product absorptive partitioning model by minimizing the square of the residuals between the observed data and the curve described by Eq. (1). The parameters α_1, α_2, $K_{\text{om},1}$, $K_{\text{om},2}$ are given in Table 2. Note that the α and K_{om} values include the effect of RH.

5.1. *Dry seed versus dry homogeneous nucleation*

Yields were determined for α-pinene oxidation by ozone in the absence and presence of initially dry seed to ascertain whether the presence or chemical composition of a dry inorganic salt affects SOA formation potential. Yield data and model fits for these experiments are given in Fig. 2. It can be seen that neither the presence of the inorganic seed nor its chemical composition has any effect on the total aerosol yield. This observation is consistent with the hypothesis that the inorganic salt does not affect gas–particle partitioning into the organic layer and acts solely as a site upon which organic deposition occurs.

5.2. *Dry seed and no seed with humid conditions*

Yield was determined at an elevated RH in the presence and absence of a dry seed, yet at an RH below that of the deliquescence points of the seed compound, for both ammonium sulfate or ammonium bisulfate. Therefore, water present in the aerosol is assumed to be associated only with the organic phase of the aerosol. Fig. 1 shows yield data obtained for these experiments, including the effect of aerosol water uptake.

Fig. 3 shows the organic aerosol yield obtained under dry seed conditions at elevated RH, as well as the

Table 1
Experimental results

Date	Δ(α-pinene) (μg m^{-3})	$\Delta M_{\text{org+water}}$ (μg m^{-3})[a]	O_3 (ppb)	RH (%)	Temp (°C)	Yield (%)	Seed type	Condition	Amount (mol m^{-3})[b]
11/29a	411	82	280	<2	28	20.0	$(NH_4)_2SO_4$	Dry	2.0×10^{-7}
11/29b	792.8	190	360	<2	28	24.0	$(NH_4)_2SO_4$	Dry	1.2×10^{-7}
12/03a	223.3	34	370	<2	28	15.2	$(NH_4)_2SO_4$	Dry	1.7×10^{-7}
12/03b	398.1	79	315	<2	28	19.8	$(NH_4)_2SO_4$	Dry	1.9×10^{-7}
12/06b	125.8	10	280	<2	28	7.9	$(NH_4)_2SO_4$	Dry	2.3×10^{-7}
12/16b	562.1	83	580	62	29.3	14.8	NH_4HSO_4	Aqueous	1.2×10^{-7}
12/17a	204.9	10	242	54.9	28	4.9	NH_4HSO_4	Aqueous	1.4×10^{-7}
12/17b	404.8	53	258	56.6	28	13.1	NH_4HSO_4	Aqueous	2.9×10^{-7}
12/18a	416	51	255	45	27.3	12.3	NH_4HSO_4	Aqueous	4.1×10^{-7}
12/18b	659.7	108	410	52.5	27.3	16.4	NH_4HSO_4	Aqueous	2.2×10^{-7}
12/19a	90.9	3	201	56.3	26.8	3.3	NH_4HSO_4	Aqueous	2.2×10^{-7}
12/19b	828.5	175	452	53.9	26.8	21.1	NH_4HSO_4	Aqueous	2.4×10^{-7}
12/21a	365.5	9.9	233	45.1	27.6	2.7	$(NH_4)_2SO_4$	Aqueous	1.9×10^{-7}
12/21b	900.9	148	302	52.4	27.6	16.4	$(NH_4)_2SO_4$	Aqueous	1.9×10^{-7}
01/03a	69	1.5	330	48.5	27.6	2.2	$(NH_4)_2SO_4$	Aqueous	1.7×10^{-7}
01/03b	384.4	35	350	48.1	27.6	9.1	$(NH_4)_2SO_4$	Aqueous	1.9×10^{-7}
01/04a	753.8	125	310	48.5	29.2	16.6	$(NH_4)_2SO_4$	Aqueous	2.4×10^{-7}
01/04b	571.5	79	208	55.2	29.2	13.8	$(NH_4)_2SO_4$	Aqueous	1.8×10^{-7}
01/05a	1302.3	263	310	47.1	28	20.2	$(NH_4)_2SO_4$	Aqueous	2.5×10^{-7}
01/05b	1183.5	216	280	50	28	18.3	$(NH_4)_2SO_4$	Aqueous	1.5×10^{-7}
01/08a	398.5	80	270	<2	27.8	20.1	None	N/A	0
01/10a	225.2	35	278	<2	28.9	15.5	None	N/A	0
01/10a	512.5	110	499	<2	28.9	21.5	None	N/A	0
01/11a	386.3	86	250	41	28.8	22.3	None	N/A	0
01/11b	675	177	380	57.7	28.8	26.2	None	N/A	0
01/12a	235.9	45	205	31	29.5	19.1	None	N/A	0
01/12b	686.7	175	258	46	29.5	25.5	None	N/A	0
01/13a	396	79	244	14.1	29.5	19.9	NH_4HSO_4	Dry	0.7×10^{-7}
01/13b	648.4	145	352	14.4	29.5	22.4	NH_4HSO_4	Dry	1.5×10^{-7}
01/14a	265	48	402	14.6	29.6	18.1	NH_4HSO_4	Dry	1.9×10^{-7}
01/14b	541.1	115	313	16.6	29.6	21.3	NH_4HSO_4	Dry	1.8×10^{-7}
01/17a	986.5	281	324	37.3	29.7	28.5	None	N/A	0
01/18a	636.6	140	130	<2	29.1	22.0	$(NH_4)_2SO_4$	Dry	2.0×10^{-7}
01/19a	389.2	74	256	39	29.4	19.0	$(NH_4)_2SO_4$	Dry	2.4×10^{-7}
01/19b	848.2	213	503	49	29.4	25.1	$(NH_4)_2SO_4$	Dry	3.3×10^{-7}
01/20a	189.7	25	190	45.3	29	13.2	$(NH_4)_2SO_4$	Dry	4.1×10^{-7}
01/20b	669.3	165.5	600	49.2	29	24.7	$(NH_4)_2SO_4$	Dry	1.9×10^{-7}
01/21a	627.1	98	180	47.1	29.7	15.6	$(NH_4)_2SO_4$	Aqueous	1.4×10^{-7}
01/21b	964.5	165	206	50.2	29.7	17.1	$(NH_4)_2SO_4$	Aqueous	2.1×10^{-7}
01/22a	888.5	220	175	<2	29.6	24.8	None	N/A	0
01/22b	762.6	185	380	<2	29.6	24.3	None	N/A	0
01/24a	406	60	250	41.5	28.5	14.8	$CaCl_2$	Aqueous	2.7×10^{-7}
01/24b	628.2	130	300	57.5	28.5	20.7	$CaCl_2$	Aqueous	2.9×10^{-7}
01/25a	256.3	25	260	49.2	29.5	9.8	$CaCl_2$	Aqueous	0.97×10^{-7}
01/25b	623.7	120	300	50	29.5	19.2	$CaCl_2$	Aqueous	2.2×10^{-7}
01/26a	1204.3	295	153	43.9	29	24.5	$CaCl_2$	Aqueous	1.6×10^{-7}
01/26b	933.9	215	246	51.2	29	23.0	$CaCl_2$	Aqueous	1.5×10^{-7}

[a] The increase in aerosol mass caused by the uptake of organic matter and net change in liquid water content. Calculated from Eqs. (3) and (4).

[b] The quantity of salt seed listed here was estimated from the observed size distribution as described in Section 6.1. It is the amount of aerosol in the chamber 60 min after O_3 injection, and corresponds to the quantities V_{salt} in Eq. (3) and $V_{\text{salt+water}}$ (when associated with the equilibrium amount of liquid water) in Eq. (4).

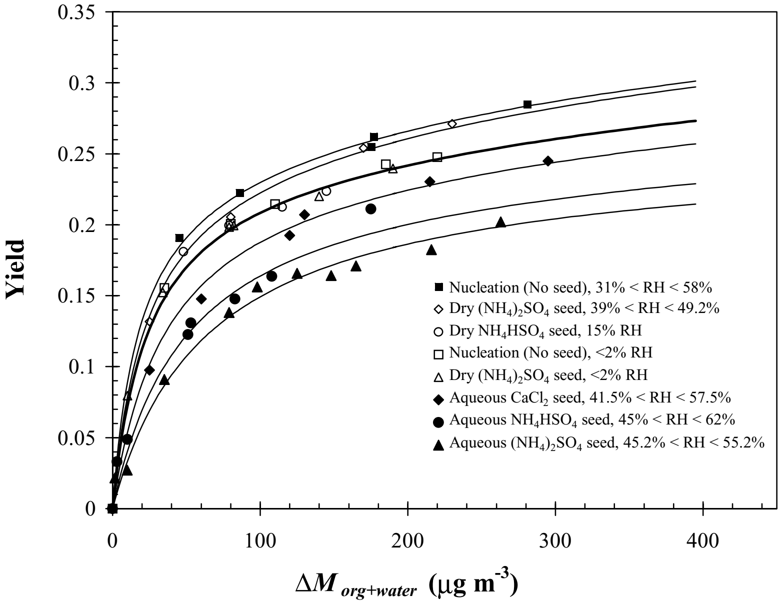

Fig. 1. Summary of experimental yield data. Yields have not been corrected for water uptake, and the $\Delta M_{\mathrm{org+water}}$ is the increase in mass of the aerosol in the chamber assuming the density of the aerosol is $1\,\mathrm{g\,cm^{-3}}$. Solid line is two-product fit through each data set. The thick line is the two-product fit through both the low RH nucleation and the low RH, dry seed experiments. Exact RH for each data point are given in Table 1.

Table 2
Empirically fit partitioning coefficients

Experimental conditions	α_1	α_2	$K_{\mathrm{om},1}$ ($\mu\mathrm{g\,m^{-3}}$)	$K_{\mathrm{om},2}$ ($\mu\mathrm{g\,m^{-3}}$)
Dry nucleation	0.239	0.169	0.042	0.0010
Wet nucleation before water correction	0.239	0.169	0.056	0.0019
Wet nucleation after water correction	0.239	0.169	0.042	0.0010
Dry $(NH_4)_2SO_4$	0.239	0.169	0.042	0.0010
Dry NH_4HSO_4	0.239	0.169	0.042	0.0010
RH 50%, dry $(NH4)_2SO_4$ before water correction	0.239	0.169	0.046	0.0018
RH 50%, dry $(NH4)_2SO_4$ after water correction	0.239	0.169	0.042	0.0010
RH 50%, aqueous $(NH_4)_2SO_4$	0.239	0.169	0.016	0.00013
RH 50%, aqueous NH_4HSO_4	0.239	0.169	0.020	0.00028
RH 50%, aqueous $CaCl_2$	0.239	0.169	0.028	0.00073

aerosol yield obtained in the absence of seed aerosol at elevated RH, all corrected for the water uptake of the organic phase of the aerosol. After correcting for water uptake, it can be seen that the measured yields in all of these experiments fall onto the same curve obtained for the dry experiments. This result demonstrates again that the dry inorganic seed aerosol does not influence the gas–particle conversion processes occurring, even at elevated RH. This observation is further supported by the fact that there are no discernible changes in the aerosol yield parameters between experiments in which the aerosol is produced by homogeneous nucleation and those with dry seed particles present. The fact that the organic aerosol yields are similar to those of the dry experiments implies that the distribution and volatility of the organic oxidation products have not been significantly altered by the presence of water. Aerosol yield formation parameters determined for α-pinene/O_3 under dry conditions are therefore sufficient to describe the gas–particle partitioning under humid conditions, as long as none of the water is associated with the inorganic seed aerosol.

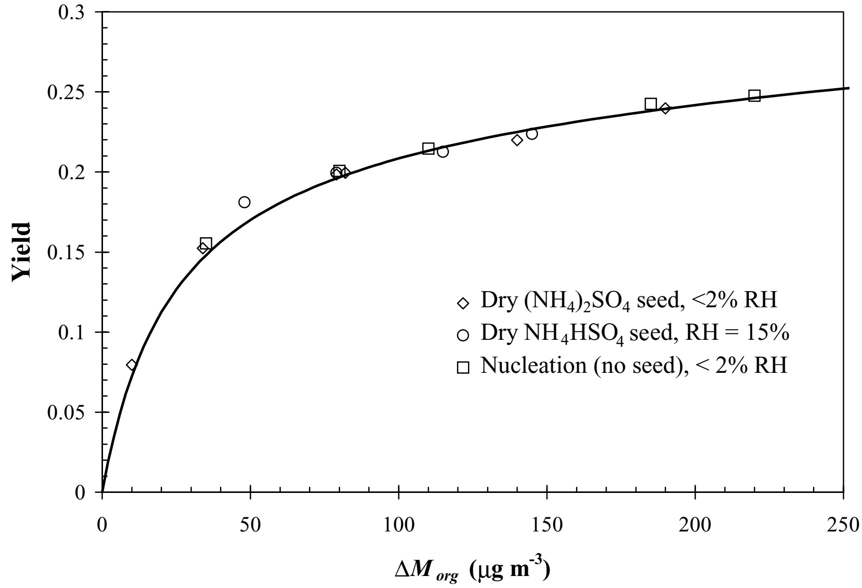

Fig. 2. Summary of experimental yield data taken under dry conditions (RH < 2%) in the presence of dry $(NH_4)_2SO_4$, dry NH_4HSO_4, and no seed present. Solid line is two-product fit of data to Eq. (1): $\alpha_1 = 0.239$, $K_{om,1} = 0.042\,m^3\,\mu g^{-1}$, $\alpha_2 = 0.169$, $K_{om,2} = 0.001\,m^3\,\mu g^{-1}$.

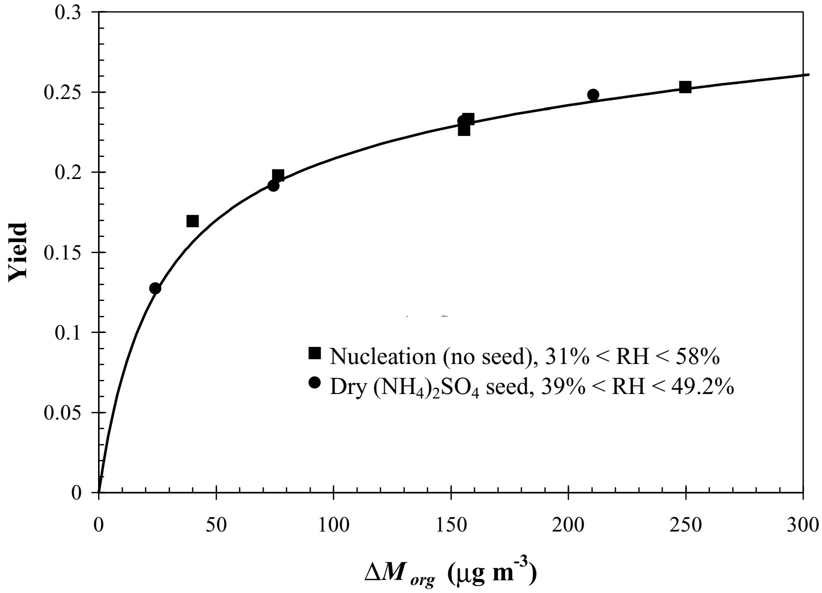

Fig. 3. Aerosol yield corrected for water uptake of organics for nucleation at RH = 50% and for $(NH_4)_2SO_4$ seed aerosol, dry, at RH = 50%. Solid line is from Fig. 2. Exact humidities for each data point are given in Table 1.

5.3. *Aqueous salt solutions effect on SOA yield*

Aerosol formation potentials were measured at elevated RH for α-pinene oxidation by ozone in the presence of aqueous $(NH_4)_2SO_4$, NH_4HSO_4, and $CaCl_2$ seed aerosol. Yields for all three salts are given by the lowest three curves in Fig. 1. These curves include the total mass absorbed by the aerosol, which includes both organic and water constituents. Yield curves for all three aqueous salt systems were below those of the baseline dry curve as well as the yield curves at elevated humidity with dry seed.

Correction for water uptake of the aqueous aerosol is necessary to make a direct comparison of the organic aerosol formation in the dry and wet cases. Although the water associated with the salt alone can be calculated, and the water associated with the organic can be obtained through TDMA measurements, estimation of the water content of the composite aerosol is confounded by the organic–inorganic–water interactions. Several observations can be made even before attempting to remove the water content of the aerosol from the raw data. The presence of the electrolytes clearly reduces the fraction of organic aerosol partitioning from the gas to the aerosol phase. Secondly, the hygroscopic water uptake by the organic compounds themselves is not sufficiently large to produce as much total aerosol (organic and water) as organic aerosol is formed in the dry experiments. Finally, and most interestingly, the reduction in aerosol production is dependent on the composition of salt in aqueous form.

5.4. *Hygroscopic properties of α-pinene/ozone aerosol products*

The hygroscopic behavior of an aerosol is typically reported in terms of a growth factor, G_f, which is defined as the ratio of the humidified diameter ($D_{p,\mathrm{w}}$) to the dry aerosol diameter ($D_{p,\mathrm{d}}$), and conventionally measured using a tandem differential mobility analyzer (McMurry and Stolzenburg, 1989)

$$G_f = D_{p,\mathrm{w}}/D_{p,\mathrm{d}}. \tag{5}$$

Table 3 reports the G_f values determined for each of the inorganic seed compounds at 85% RH, as well as theoretically predicted values (see Section 6.1). The agreement with predicted values provides confidence in our assignment of the state of the aerosol, i.e. deliquesced or effloresced. G_f did not vary appreciably for size-classified particles of 136 and 235 nm diameter.

Table 3
Hygroscopic growth factors obtained from TDMA measurements

Compound	Initial RH	Final RH	Growth factor	
			Measured	Predicted
α-Pinene SOA[a]	<2%	50%	1.04	—
α-Pinene SOA[a]	<2%	85%	1.09[b]	—
Dry $(NH_4)_2SO_4$	<2%	85%	1.58	1.58
Dry $(NH_4)_2SO_4$	50%	85%	1.59	1.58
Aqueous $(NH_4)_2SO_4$	50%	85%	1.31	1.28
Dry NH_4HSO_4	<2%	85%	1.65	1.64
Aqueous NH_4HSO_4	50%	85%	1.36	1.33
Aqueous $CaCl_2$	50%	85%	1.31	1.29

[a] Measured at 180 min after the start of the experiment.

[b] Virkkula et al. (1999) reports a growth factor of 1.08 at 85%.

Growth factors were measured for the dry seed (<2% RH) system during the course of reaction as ammonium sulfate became progressively coated with organic products of α-pinene/O_3 oxidation. The TDMA was set to 85% RH with either 136 or 235 nm diameter chamber aerosol being selected for the hygroscopic growth. Analysis of the TDMA data followed that of Virkkula et al. (1999), where the hygroscopic uptake of the aerosol can be described by treating the inorganic and organic uptake of water separately,

$$G_f = \varepsilon_1 G_{f(1)}^3 + (1 - \varepsilon_1) G_{f(2)}^3, \tag{6}$$

where ε_1, $G_{f(1)}$ and $G_{f(2)}$ refer to the fraction of organic present in the aerosol and the growth factors of the pure organic and inorganic portions, respectively. The organic volume fraction is calculated from the relative volume of dry aerosol to aerosol at the time of measurement. Fig. 4 shows the evolution of G_f as a function of the organic fraction of the aerosol. Table 3 presents the growth factors of the organic and inorganic fractions at different RHs. The growth factors determined for the aerosol formed in α-pinene oxidation by ozone are similar with those of the less hygroscopic mode measured in ambient aerosols (Svenningsson et al., 1992; Ferron et al., 1999; Massling et al., 1999; Swietlicki et al., 1999; Cocker et al., 2001b). No discernible differences were seen in the growth factors of the 136 and 235 nm diameter particles. It was assumed that the growth factor of the organic fraction remains constant over the 4-h period of growth.

The TDMA data clearly demonstrate that the coating of inorganic particles with organic compounds reduces the hygroscopic nature of the aerosol. The close fit of the data to Eq. (6) shows that for the α-pinene/ozone system, accounting for the organic and inorganic water uptake separately can approximate the G_f of the organic–inorganic aerosol. A more rigorous treatment of the water–inorganic–organic interactions in this system are treated in detail in Section 6.

Growth factors determined in the TDMA experiments were used to estimate the volumetric fraction of water taken up by organic aerosol during experiments in which the RH was 50% and the seed, when present, was dry. Aerosol produced during dry nucleation experiments (0 water, purely organic in content) was humidified in the TDMA as a surrogate for what occurs in the chamber during humid nucleation experiments. Aerosol produced during the dry seed, 0 RH (RH<2%) experiments (0 water on aerosol) were humidified to 50% (below the deliquescence point of the seed) and the uptake of water by the organic was measured.

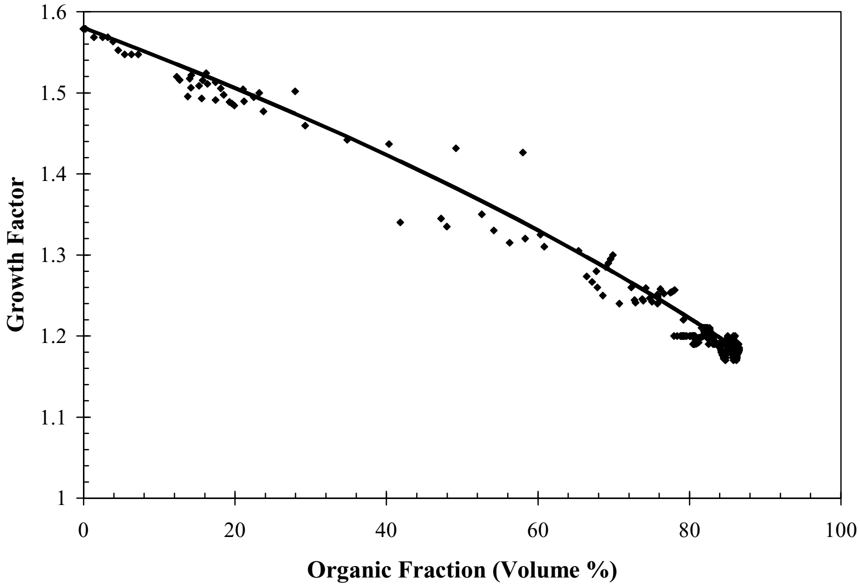

Fig. 4. Growth factors (Gf) for α-pinene/O3 SOA from dry conditions to 85% RH (Experiment 12/6/1999) as a function of the organic fraction of the aerosol.

6. Thermodynamic modeling of gas–aerosol equilibria

We now examine the possibility of explaining theoretically the experimental observations just presented. At the outset it should be noted that thermodynamic data for organic/inorganic/water systems of the type considered are scant; therefore, there is little at present on which to base a rigorous test of the accuracy of a thermodynamic theory. The UNIFAC model (Fredenslund et al., 1975; Hansen et al., 1991) has been used to estimate activity coefficients for organic/water aerosol mixtures (Saxena and Hildemann, 1997; Ansari and Pandis, 2000; Zhang et al., 2000), and is employed here in some calculations. The approach proposed by Clegg et al. (2001) is used for predicting activity coefficients in solutions containing water, dissolved organic compounds, and salts. In this method, activity and osmotic coefficient (water activity) contributions are first calculated separately for the salt/water and organic/water components of the liquid-phase. These are combined with terms expressing mixture effects ("salting in" and "salting out") to produce thermodynamically self-consistent estimates of the activity and osmotic coefficients in the mixture.

The oxidation of α-pinene by ozone was previously studied by Yu et al. (1999) who determined the yields of the main products (see their Table XI). In this work we take the average of the two experiments reported by Yu et al. (1999) performed on 9 June 1998. Compound vapor pressures have been estimated using the method of Myrdal and Yalkowsky (1997), though with some further optimization based on the results of the present experiments.

6.1. Salt aerosols

The water activity, a_w, of an aqueous solution may be written as (Robinson and Stokes, 1959),

$$a_w = \exp\left(-(M_w/1000)\phi \sum_i m_i\right), \tag{7}$$

where M_w is the molecular weight of pure water, ϕ is the practical osmotic coefficient of the solution, and m_i is the molality of ion or solute molecule i. For droplets of a size sufficiently large that corrections for surface curvature can be neglected, the RH (in %) and the water activity are related by $\mathrm{RH} = 100a_w$. As $\sum_i m_i$ approaches zero (corresponding to pure water) the value of ϕ tends to unity.

Water activities of aqueous solutions of the salts $(NH_4)_2SO_4$, NH_4HSO_4 and $CaCl_2$ are required and were obtained as follows. For $(NH_4)_2SO_4$, the model of Clegg et al. (1995) was used. This is based upon osmotic coefficients (measured for bulk solutions) up to the saturation concentration of about 5.8 mol kg^{-1} (80% RH), and electrodynamic balance data to >25 mol kg^{-1} (about 40% RH). Osmotic coefficients of aqueous NH_4HSO_4 were calculated using the model of Clegg et al. (1998b), which is also based upon extensive measurements to very low RH. The equations of Anathaswamy and Atkinson (1985) were used for

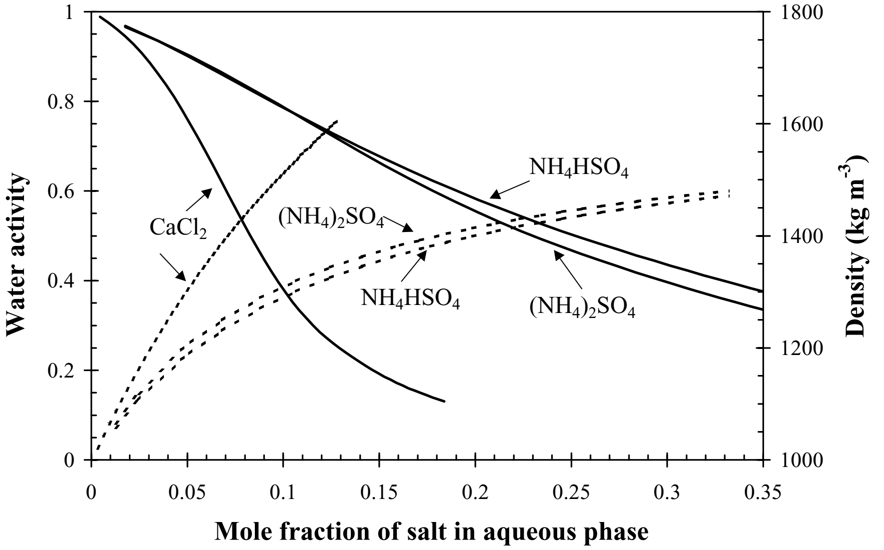

Fig. 5. Equilibrium water activity, equal to RH (solid lines), and density (dashed lines) for three aqueous salt solutions as a function of aqueous-phase salt mole fraction.

aqueous $CaCl_2$. Densities for aqueous $CaCl_2$ were calculated using the expression given by Sohnel and Novotny (1985); densities for aqueous $(NH_4)_2SO_4$ and NH_4HSO_4 were taken from Tang and Munkelwitz (1994). The dependence of water activity and density on solution concentration at 301 K is shown in Fig. 5 for the three salts.

6.2. Water uptake by condensed organic material

TDMA-measured growth factors for the α-pinene SOA and the three salts are listed in Table 3, and growth factors for mixtures of the organic products with $(NH_4)_2SO_4$ are shown in Fig. 4. Measured growth factors for the pure salts are compared directly with those calculated from literature osmotic coefficient and density data in Table 3. There is reasonable agreement for all three salts. We note that, at 85% RH, the RH in the TDMA is controlled to within +2%. This might be the cause of the small difference between the measured and calculated growth factor for $CaCl_{2(aq)}$.

We first consider water uptake by the α-pinene oxidation products alone. It is assumed that both the compounds themselves and their solutions in water have unit density, thus

$$M_{\text{org+water}}/M_{\text{org}} = G_f^3, \tag{8}$$

where $M_{\text{org+water}}$ is the total mass of organic material plus water, M_{org} is the mass of the organic material alone, and G_f is the growth factor from dry conditions to some known RH. Expressing the total mass as the sum of the organic and water masses, the number of moles of condensed water, nH_2O, is

$$nH_2O = (G_f^3 - 1)M_{\text{org}}/18.0152. \tag{9}$$

Assuming that the organic composition of the aerosol remains constant over the course of the oxidation, the mean molar mass of condensed-phase organic material is predicted to be 184 g mol^{-1} (see Section 6.3.1). Using this value enables the mean mole fraction of the condensed organic material, and that of water, to be calculated from the measured growth factors using Eq. (9).

The growth factors are determined by subjecting an aerosol, under initially dry conditions, to an increased RH and measuring the change in the aerosol size distribution. Deliquescence would be expected to be observed in the case of a mixed salt aerosol, which would remain solid or retain a solid fraction, at RHs below the deliquescence RHs of the various components. Similarly, it is possible that not all of the organic material dissolves in the present experiments, and we must consider this possibility in our analysis.

Calculated total mole fractions of dissolved organic material at 50% and 85% RH, based upon the growth factor measurements, are shown in Fig. 6 for two different assumptions: first, that the organic aerosol is fully liquid and, second, that only about half of the organic material has dissolved in the aerosol water. For the latter case the exact figure is 53% dissolved—this was chosen as it corresponds to Raoult's law behavior of the liquid part of the aerosol at 85% RH. For simplicity, we assume that the same fraction is dissolved at 50% RH although in general the value would be expected to

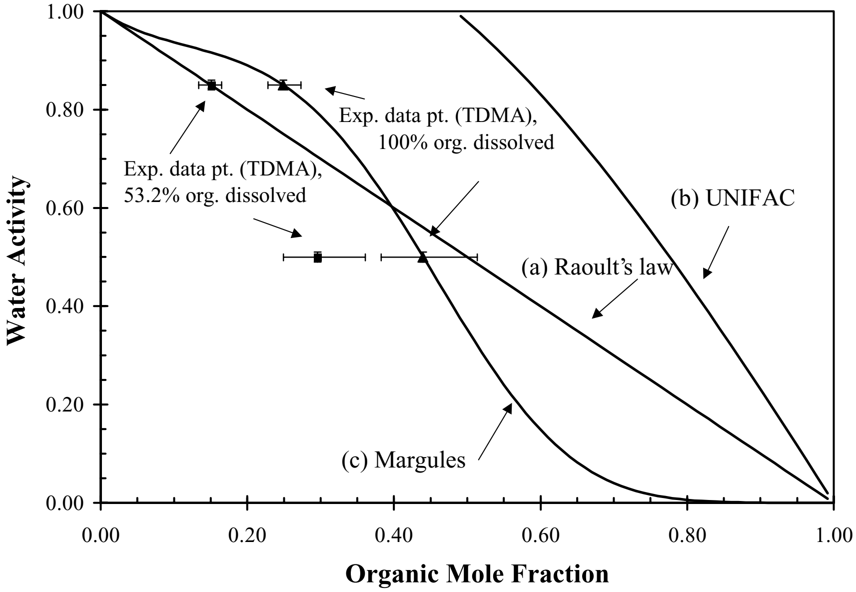

Fig. 6. Equilibrium water activity, equal to RH, for mixtures of α-pinene SOA and water as a function of liquid-phase mole fraction of SOA. Curve (a) assumes Raoult's law solution behavior; curve (b) uses UNIFAC to predict equilibrium water activity; curve (c) uses a Margules 2-parameter best fit ($\ln \lambda_{\mathrm{water}} = (w + 3u)\gamma^2_{\mathrm{org}} - 4ux^3_{\mathrm{org}}$, $w = -4.777$, $u = 3.38038$). Data points shown are from TDMA growth measurements assuming a ±0.01 G_{f} error with either complete organic dissolution or 53.2% dissolution of organic.

be lower (which would displace the data point to the left). The simplest assumption is that the water uptake obeys Raoult's law (see curve (a)), hence the water mole fraction in the liquid phase is equivalent to the RH. This is broadly consistent with the data, though the measured water uptake at 85% RH is less than predicted if we assume that the organic material is fully dissolved. However, even without this assumption, Raoult's law provides a much better prediction than does UNIFAC for the condensed phase compounds. This model, curve (b), underestimates the amount of water uptake by a large margin: at 80% RH UNIFAC predicts 0.9 mol $H_2O\,\mathrm{mol}^{-1}$ of total organic compounds for a fully liquid aerosol compared to a measured value of about 3 mol of H_2O. Curve (c) represents a two-parameter Margules model fitted to the data for 50% and 85% RH, and assuming a fully liquid aerosol. If the organic compounds are treated as a single solute then its activity, as calculated by this model, is only about 0.05 at 50% RH. This is a factor of 10 lower than given by Raoult's law. In a system in which the organic component is volatile then the two-parameter Margules model implies much greater partitioning into the condensed phase than Raoult's law for all RH > 0. The same is likely to be true of most models based upon the two points in Fig. 2 that assume limited solubility of the organic component.

Next, we examine the extent to which measured growth factors for mixtures of α-pinene oxidation products and $(NH_4)_2SO_4$ (Fig. 4) can be explained based on thermodynamic theory. Osmotic coefficients, ϕ, of the mixture (hence, by iteration, the water content) are estimated using Eq. (3) of Clegg et al. (2001), which reduces to:

$$\phi = 1 + \frac{3(\phi' - 1)m_{\mathrm{salt}}}{\Sigma_i m_i} + \frac{(\phi'' - 1)m_{\mathrm{org}}}{\Sigma_i m_i} + \frac{2m_{\mathrm{salt}}m_{\mathrm{org}}\lambda_{\mathrm{org,\,salt}}}{\Sigma_i m_i}, \tag{10}$$

where m indicates molality, ϕ' is the osmotic coefficient contribution from the $(NH_4)_2SO_4$/water component of the solution, and ϕ'' is the contribution from the organic/water component. The last term in Eq. (10) is the contribution from ion–organic interactions ("salting in" or "salting out"), characterized by the parameter $\lambda_{\mathrm{org,\,salt}}$. The $\Sigma = \left(3m_{\mathrm{salt}} + m_{\mathrm{org}}\right)$. It is assumed that the apparent molar volumes of both the $(NH_4)_2SO_4$ and dissolved organic material are the same in their aqueous mixtures as in pure (single solute) solutions at the same molality.

It is important to realize that although the salt effect generally refers to the change in solubility of a volatile solute due to presence of salts in the solution, the corresponding influence on the osmotic coefficient shown in Eq. (10) can be important when the concentration of the volatile solute in the condensed phase is comparable to that of the salt. Salting out, for which the parameter $\lambda_{\mathrm{org,\,salt}}$ is positive, decreases the water activity of a solution, which has the effect of increasing water

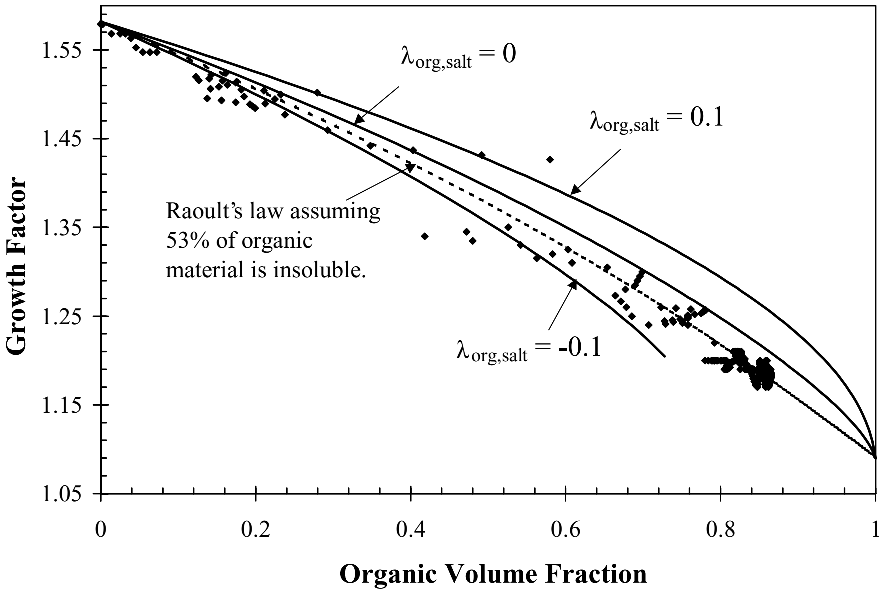

Fig. 7. Measured and calculated growth factors at 301 K for aerosols containing a mixture of organic compounds and $(NH_4)_2SO_4$. Symbols—data from experiment 12/6/1999 (Fig. 4). Dashed line is predicted using Raoult's law to calculate equilibrium and 53.2% organic dissolution. Solid lines use two-component Margules model (Fig. 6) using $\lambda_{\text{org, salt}} = -0.1$, 0.0, $+0.1$.

uptake into the condensed phase in a system at a fixed RH. Consequently, because of a greater volume of solvent, the partitioning of the volatile compound into the liquid phase is enhanced, thus counteracting the decrease in its solubility. The extent to which these two effects cancel each other determines the overall partitioning that occurs in any given situation.

In Fig. 7, growth factors for the organic/$(NH_4)_2SO_4$ mixtures are compared with two sets of predictions: first, with organic/water osmotic coefficient contributions ϕ'' predicted using the two component Margules model (Fig. 6). For this case, we also show growth factors calculated with $\lambda_{\text{org, salt}} = -0.1$ (salting in) and $+0.1$ (salting out). Second, predicted growth factors are plotted that assume Raoult's law organic/H_2O activities, and 53% of the organic material insoluble (in order to match the measured growth factor at 85% RH as noted previously). We note that growth factors for this case but with non-zero $\lambda_{\text{org, salt}}$ (not shown) are similar to those for the two component Margules model, in that they fall on either side of the plotted line for the $\lambda_{\text{org, salt}} = 0$. However, the magnitude of the effect is smaller as the amount of soluble organic material is less.

It is clear that measured and predicted growth factors of the mixed solutions in Fig. 7 for both cases agree most closely when $\lambda_{\text{org, salt}} = 0$, although the best result is obtained for the calculation assuming limited solubility of the organic matter. If the total amount of water in the condensed phase is assumed to be equal to the sum of the amounts that would be taken up by the salt and organic compounds separately, then both calculations give essentially the same result as Eq. (6) as would be expected.

6.3. *Theoretical analysis of measured aerosol yields*

We now address the extent to which it is possible to explain the observed aerosol yields using thermodynamic models. In doing so, we consider both a two-product model of the organic aerosol and a multi-product model based on product compounds identified by Yu et al. (1999). For each model, we first address the yields observed in the absence of seed aerosol under dry conditions and at 50% RH. Then, for each model, we consider the yields observed in the presence of a wet seed aerosol.

6.3.1. *Two-product aerosol model*

In the two-product model given by Eq. (1), the organic compounds that form SOA are treated as two classes: one that partitions chiefly into the particle phase (and is relatively involatile), and a second class of more volatile compounds that remain mainly in the gas phase. The two partitioning coefficients $K_{\text{om},1}$ and $K_{\text{om},2}$ are equivalent to equilibrium constants for the two compound classes, though with the use of mass fraction rather than mole fraction as the condensed phase concentration varies. It is clear from the fits in Fig. 1 that Eq. (1) represents the experimental data well.

The model is based upon the $\alpha_{1,2}$ and $K_{\mathrm{om},1,2}$ values for dry nucleation without salts (Table 2). Mean molar masses of the involatile and volatile compound classes are taken as 184 and 169 g mol^{-1}, respectively (see Section 6.3.2 below). On a molar basis, α_1 is then equal to 0.177, and α_2 is 0.136, giving 0.313 mol of total organic products per mole of α-pinene. This is very close to the 0.309 average of the results 6/9/98a, b obtained by Yu et al. (1999). The partition coefficients are converted to mole-fraction based equilibrium constants given by,

$$K_{x,i} = x_i f_i / p_i, \tag{11}$$

where *i* represents each of the organic compound classes, distributed between the gas phase and a liquid aerosol phase that can also contain water and salts, *x* indicates the mole fraction, p_i the equilibrium partial pressure (atm), and f_i is the mole fraction based activity coefficient of *i*, which has a value of unity for pure *i*. The activity coefficients of the two organic compound classes are assumed to be the same in all solutions, and both equal to unity in a mixture in which there are no other components.

Table 4
Phase partitioning predicted from Eq. (1)[a]

Compound	Experiment I mass (μg m^{-3})[b]	Experiment II mass (μg m^{-3})[b]
Δ(α-Pinene)	888.5	236.6
Component 1 (aerosol)[c]	191.6	33.7
Component 1 (gas)	20.7	22.9
Component 2 (aerosol)[d]	28.4	1.35
Component 2 (gas)	121.8	38.6

[a] For 2% RH and 301 K.

[b] Experiments I and II refer to two experiments performed by Yu et al., 1999 on 9 June 1998.

[c] "Involatile" products.

[d] "Volatile" products.

Values of $K_{x,i}$ for each compound class were estimated by solving Eq. (1) to obtain the gas-phase and particulate amounts of both product classes (Table 4), and then converting condensed phase mass fractions to mole fractions and gas-phase amounts to partial pressures. Thus $K_{x,1} = 3.1 \times 10^8$ atm^{-1}, and $K_{x,2} = 7.6 \times 10^6$ atm^{-1}.

First, we consider the effect of water on the partitioning of the organic compounds. Calculations using UNIFAC for a mixture of water and the product compounds listed in Table 5 suggest that the activity coefficient of water is increased in the organic/water mixture. This would result in a lower mole fraction of water in the aerosol phase than predicted by Raoult's law. We have used the two-component model described above, together with Eq. (10), to estimate total yields for various assumed properties of the condensed organic/water mixtures. Fig. 8a shows the measured yields for an organic/water system, without salt seed, at 2% and 50% RH, together with predictions assuming a fully liquid aerosol and Raoult's law behavior of the condensed phase. The predicted yield for 50% RH is too high by a large margin. How can this be explained? First, the true values of the activity coefficients of the organic components and/or water may be greater than unity in the aerosol. These changes would lead to a greater

Table 5
Products of the oxidation of α-pinene by ozone

Compound[a]	Formula	Yield[b]	p^o (301 K)[c]
Pinic acid (A2)	$C_9H_{14}O_4$	4.50	1.5×10^{-8}
Norpinic acid (A1)	$C_8H_{12}O_4$	0.10	8.1×10^{-8}
Hydroxy pinonaldehyde (A12)	$C_{10}H_{16}O_3$	2.85	7.7×10^{-7}
Pinonic acid (A6)	$C_{10}H_{16}O_3$	2.35	3.6×10^{-7}
Norpinoic acid (A5)	$C_9H_{14}O_3$	7.25	1.1×10^{-6}
Pinonaldehyde (A9)	$C_{10}H_{16}O_2$	8.20	3.7×10^{-5}
Norpinonaldehyde (A9)	$C_9H_{14}O_2$	1.45	1.6×10^{-4}
2,2-Dimethyl-cyclobutyl-1,3-dicarboxaldehyde (A8)	$C_8H_{12}O_2$	0.35	3.3×10^{-4}
Hydroxy pinonic acid (A7)	$C_{10}H_{16}O_4$	2.20	1.1×10^{-8}
(2,2-Dimethyl-3-acetyl)-Cyclobutyl formate (A3)	$C_{10}H_{16}O_3$	1.05	6.1×10^{-6}
A13[d]	$C_{10}H_{14}O_4$	0.12	3.2×10^{-7}
A14[d]	$C_{10}H_{14}O_4$	0.55	3.2×10^{-7}

[a] The numbers in parentheses refer to the product numbers of Yu et al. (1999).

[b] The product yield in mol% of the α-pinene reacted.

[c] The estimated vapor pressure (Myrdal and Yalkowsky, 1997), in atmospheres, of the pure compound as a supercooled liquid. These values were reduced by a factor of 100 in the calculations (see text).

[d] In Table VI of Yu et al. (1999) compound A13 has been erroneously assigned the same structure as A3. Here we assume that A13 is similar to A14, but with the C = O group next to the –CHO swapped with the CH_2 preceeding the –COOH. The UNIFAC group compositions of these minor oxidation products are the same.

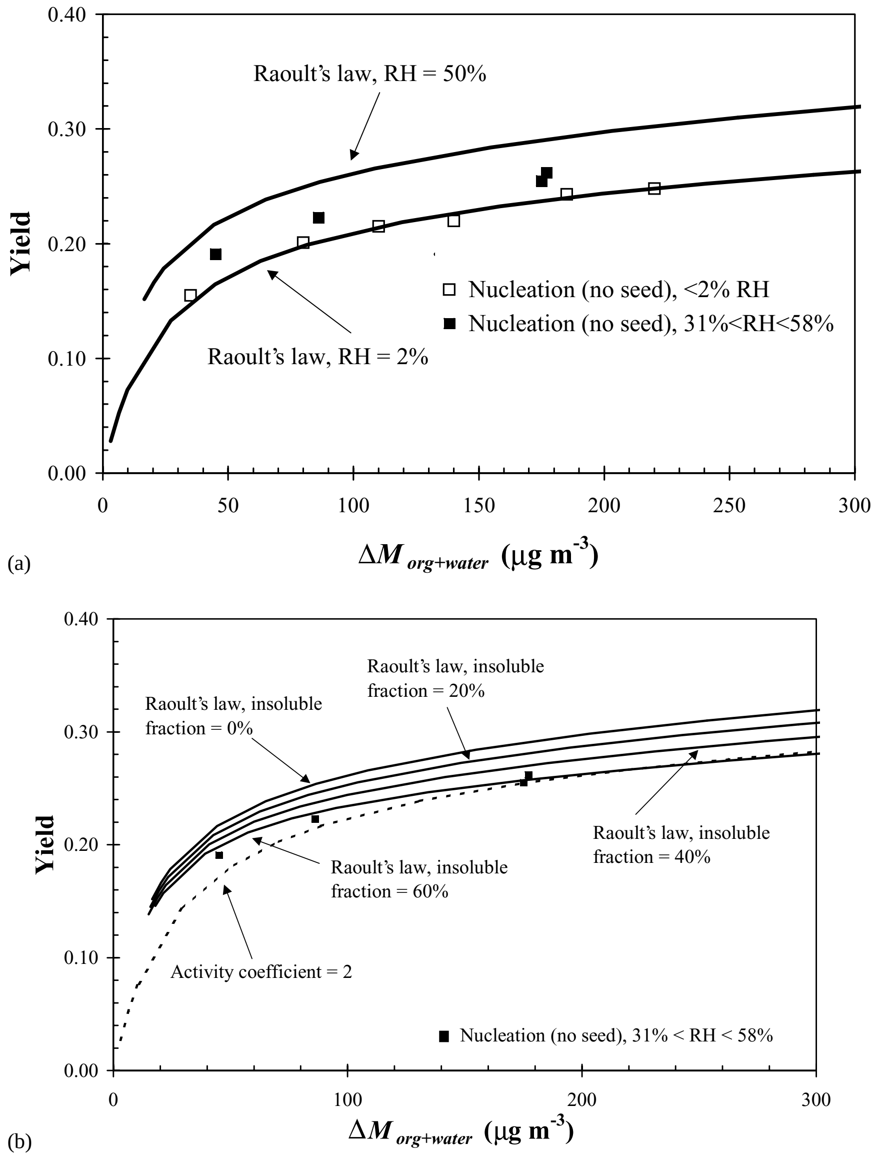

Fig. 8. Measured and calculated yields for organic/water system with no salt seed, at 2% and 50% RH. Symbols—all data under these conditions, see Table 1 for exact RH for each data point. (a) Solid line—predicted aerosol yield assuming fully liquid aerosol and Raoult's law behavior. (b) Dashed line—predicted aerosol yields setting activity coefficients to 2, solid lines—predicted aerosol yield assuming Raoult's law (unit activity) and 0%, 20%, 40%, and 60% insoluble fraction.

proportion of the organic components residing in the gas phase or a lower concentration of water in the condensed phase, respectively. Second, if the condensable organic material is not fully soluble in water at 50% RH then the total aerosol yield of organic material plus water would also be reduced. Fig. 8b shows two sets of predicted yields for 50% RH: first with the organic activity coefficients arbitrarily assigned a value of 2.0 and, second, for unit activity coefficients (Raoult's law) but with various fractions of organic component 1 assumed to condense and not take up water. The measured yields can be satisfactorily matched using either assumption. However, increased activity coefficients of the organic components may be the more likely explanation, as well as being simpler, given that liquid aerosols are known to readily supersaturate with respect to dissolved constituents. The growth factors of the organic material, discussed in the previous section, are not comprehensive enough to give reliable guidance. We note also that the use of the two-parameter Margules activity coefficient model, as fitted to the 85% and 50% RH growth factors in Fig. 6, gives predicted yields at 50% RH that are too high (as the organic activity coefficients are less than unity).

Next, we consider the effect of water on SOA yield in the presence of an initially wet seed aerosol. The effect of organic partitioning to a pre-existing aqueous salt aerosol at 50% RH is to reduce the yield—by almost a third in the case of aqueous $(NH_4)_2SO_4$ (Fig. 1). If we assume a fully liquid aerosol containing the salt, dissolved organic compounds, and water, can this salt effect be explained by salting out of the organic compounds (an increase in the value of f_i)? We have calculated yield curves for 50% RH and $1.932 \times 10^{-7}\,\mathrm{mol\,m^{-3}}$ $(NH_4)_2SO_4$, for salting coefficients $\lambda_{\mathrm{org,\,salt}} = 0$ and 0.1. In these calculations, Eq. (11) is used to determine the partitioning of the two organic compound classes, and Eqs. (7) and (10) to determine the osmotic coefficient (hence water activity) of the liquid aerosol. The salt effect on the logarithm of the activity coefficient f_i is given by (Clegg et al., 2001):

$$\ln(f_i) = \ln(f_i'') + \lambda_{\mathrm{org,\,salt}} m_{\mathrm{salt}} + \ln(x_{\mathrm{w}}''/x_{\mathrm{w}}), \tag{12}$$

where $\ln(f_i'')$ is the activity coefficient of i in a solution containing only the aerosol water and dissolved organic compounds, x_w'' is the corresponding water mole fraction, m_{salt} is the molality of the salt in the liquid aerosol, and x_{w} the true water mole fraction equal to $n\mathrm{H_2O}/(n\mathrm{H_2O} + n1 + n2 + 3n(\mathrm{NH_4})_2\mathrm{SO_4})$. Fig. 9 shows that the predicted yields, for both values of $\lambda_{\mathrm{org,\,salt}}$, are substantially higher than those measured. The positive value of the salting coefficient (corresponding to a "salting out" effect) causes a predicted reduction relative to $\lambda_{\mathrm{org,\,salt}} = 0$ in the condensed yield for small amounts of α-pinene oxidized, but an increase relative to $\lambda_{\mathrm{org,\,salt}} = 0$ over most of the measured range. At low concentrations of organic compounds in the liquid aerosol, the increase in the activity coefficients of the organic compounds (which reduces their concentration in the liquid aerosol) is greater than the salt/organic influence on the osmotic coefficient Eq. (10). At high concentrations of organic compounds, the water activity relative to $\lambda_{\mathrm{org,\,salt}} = 0$ is reduced, leading to an increase in the amount of condensed phase water at equilibrium and so a higher yield overall.

The primary explanation for the behavior of the predicted yields shown in Fig. 9 is that the water associated with the salt seed provides a medium into which the organic compounds dissolve. This is also why the predicted yield is high even for very small amounts of α-pinene oxidized: most of the products partition into the pre-existing aqueous salt aerosol. These results are not sensitive to the approach used to calculate the amounts of aerosol water: the use of the Zdanovskii–Stokes–Robinson relationship in place of Eq. (10), for example, gives a yield very similar to that shown in Fig. 9. Ignoring the effect of the parameter $\lambda_{\mathrm{org,\,salt}}$ on the osmotic coefficient reduces the predicted yield considerably (not shown), but it still remains higher than the measured values for all $\Delta M_{\mathrm{org+water}}$.

Fig. 10 shows similar calculations for aqueous $CaCl_2$ seed aerosol. The predicted yields are also much higher than those measured, but vary less with the amount of α-pinene reacted than for $(NH_4)_2SO_4$. This is because, at 50% RH, the amount of water associated with the $CaCl_2\,\mathrm{mol^{-1}}$ is about three times greater than that with

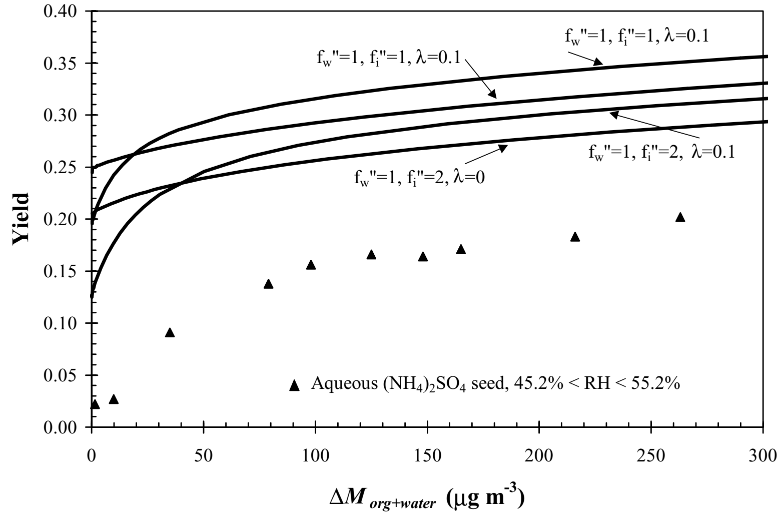

Fig. 9. Measured and calculated yields at 50% RH for systems including $1.9 \times 10^{-7}\,\mathrm{mol\,m^{-3}}$ $(NH_4)_2SO_4(aq)$ seed aerosol. Symbols—all data under these conditions. Solid lines—model prediction. f_i'' is activity of organics in solution, λ is salting parameter, see Eq. (12). Predicted yields approach zero only for very low values of $\Delta M_{\mathrm{org+water}}$.

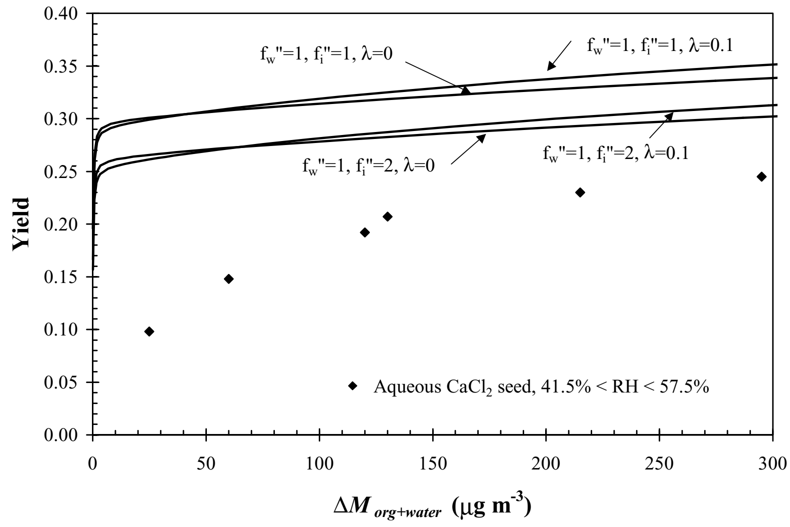

Fig. 10. Measured and calculated yield at 50% RH for systems including $1.98 \times 10^{-7}\,\mathrm{mol\,m^{-3}}$ $CaCl_2(aq)$ seed aerosol. Symbols—all data under these conditions. Solid lines—model prediction. f_i'' is activity of organics in solution, λ is salting parameter, see Eq. (12). Predicted yields approach zero only for very low values of $\Delta M_{\mathrm{org+water}}$.

$(NH_4)_2SO_4$. The salting coefficient of 0.1 has a smaller effect for $CaCl_2$ as its influence on the activity coefficient f_i is reduced due to the lower molality of the salt Eq. (12).

The fact that the measured yields are low in the presence of aqueous salt seeds, particularly for small $\Delta M_{\mathrm{org+water}}$, appears to suggest that little of the condensable organic material dissolves into the pre-existing aerosol. However, there is clearly some interaction between the salts and organic compounds, dependent upon the nature of the salt, as the yield is reduced relative to the non-seed and dry seed cases. The possibility that the observed behavior can be explained by the formation of two co-existing liquid phases—as suggested by the experiments involving pinic acid—is explored in the following section.

6.3.2. *Multi-product aerosol model*

The two-product thermodynamic model based on the empirical fit of the observed data described above quantitatively reproduces the observed aerosol formation at 2% and 50% RH for systems without salt seed aerosol. We now construct a model based upon the identified products of α-pinene oxidation (Table 5). The model is used both to interpret the results of the two-product approach, in particular to determine which compounds are likely to comprise the "involatile" and "volatile" aerosol components, and to examine the results of experiments involving aqueous salt seeds including the effects of possible liquid/liquid phase partitioning within the aerosol.

The model partitions water and each of the organic compounds in the system to achieve equilibrium between the gas and aerosol phases, thus

$$100a_{\mathrm{w}} = \mathrm{RH} \tag{13a}$$

$$p_i = x_i f_i p_i^{\mathrm{o}} \tag{13b}$$

where p_i is the gas phase partial pressure of organic compound i which is calculated from the amount present in that phase, and p_i^{o} is the vapor pressure of the pure compound as a supercooled liquid. The reference state for the activities of all solution components is the pure liquid, thus f_w approaches 1.0 as x_w approaches 1.0 and f_i approaches 1.0 as x_i approaches 1.0. Mass balance constraints for each of the organic compounds also apply. The equilibrium state of the system was determined by Gibbs energy minimization (Wexler and Clegg, 2001), rather than by solving Eqs. (13a) and (13b) simultaneously.

The UNIFAC method is used here to estimate the organic/water contributions to activity coefficients, (see Table 6 for UNIFAC group compositions) and the method of Clegg et al. (2001) is used to estimate salt effects Eq. (12). The equilibrium composition of the system was determined by Gibbs energy minimization. Pure compound vapor pressures, p_i^{o}, need to be estimated for each of the species listed in Table 5, as experimentally measured vapor pressures are not generally available for these compounds. Initial calculations showed that the estimated p_i^{o} were too high as, for most experimental conditions, no aerosol phase was predicted to exist. Accordingly, all the p_i^{o} in Table 5 were reduced

Table 6
UNIFAC (Fredenslund et al., 1975) group compositions of the oxidation products[a,b]

Compound	CH_3[c]	CH_2[c]	CH[c]	C[c]	COOH[d]	CHO[e]	CH_2CO[f]	CH_3CO[f]	OH[g]	CH_2O[h]
A2	2	2	2	1	2					
A1	2	1	2	1	2					
A12	2	2	3	2		1	1		1	
A6	2	2	1	1	1			1		
A5	2	1	2	1	1			1		
A10	2	2	2	1		1		1		
A9	2	1	2	1		1		1		
A8	2	1	2	1		2				
A7	2	2	2	1	1		1	1	1	
A3	2	1	2	1		1				1
A13	2	2	1	1	1		1			
A14	2	2	1	1	1		1			

[a] These compositions are required by UNIFAC for the calculation of the activity coefficients of the organic compounds.

[b] Each column lists the number of occurrences of the group in the molecule. See Table 5 for the chemical formulae of the compounds.

[c] Alkanes.

[d] Carboxylic acid.

[e] Aldehyde.

[f] Carbonyl.

[g] Alcohol.

[h] Ether.

by a constant factor which was adjusted (to a final value of 10^2) until reasonable agreement with the experimental yield data for RH $<2\%$ was obtained. We can compare the estimated p_i^o with recent measurements for a few compounds. Bilde and Pandis (2000) have determined the vapor pressures of pinic acid and trans-norpinic acid using a TDMA, obtaining values of 8.1×10^{-10} atm (pinic acid) and about 54×10^{-10} atm (trans-norpinic acid) at 301 K. The relative magnitudes of these vapor pressures agree well with the estimates in Table 5. However, for pinic acid, the value of p_i^o needed to reproduce the observed yield of pinic acid by Yu et al. (1999) is a factor of 5 lower than that of Bilde and Pandis (2000), and for norpinic acid a factor of almost 7. In drawing conclusions about the behavior of individual compounds, we are implicitly assuming that the relative values of p_i^o, which vary over a four order of magnitude range, are better predicted than the absolute values. Comparisons made above for pinic and trans-norpinic acids are consistent with this assumption. The effect of errors in the estimated values of p_i^o will be greatest for those compounds predicted to be present in comparable amounts in both aerosol- and gas-phases—in these cases a change in the pure compound vapor pressure can cause a shift in partitioning towards the gas phase (if p_i^o is too high) or the aerosol phase (if p_i^o is too low). Conversely, the partitioning of compounds predicted to exist almost entirely in a single phase is quite insensitive to errors in p_i^o.

Condensed phase yields for systems without salt seed aerosols, calculated using the multi-product model, are shown in Fig. 11 for both 2% and 50% RH. There is good agreement with the measurements over the full range of $\Delta M_{\text{org+water}}$ at the lower RH, as expected, but at 50% RH, the predicted yield is somewhat low. This is because the water uptake calculated using UNIFAC to obtain water activities is too low, as suggested by the growth factor measurement at 50% RH (see Fig. 6).

We next compare the results of this model with the two-product model based on Eq. (1). The partitioning of the product classes predicted by Eq. (1) for α-pinene reacted equal to 888.5 and 236.6 $\mu g\,m^{-3}$ is summarized in Table 4. For the higher α-pinene concentration, about 87 wt% of the condensed phase is predicted to be composed of the mainly non-volatile component 1, while component 2 makes up 81 wt% of the total organic products present in the gas phase. For Δ(α-pinene) $=236.6\,\mu g\,m^{-3}$, the smaller amounts of the two product components reflect the shift in partitioning towards the gas-phase; here only 59.5% of component 1 is predicted to reside in the condensed phase, while 96.6% of component 2 is predicted to exist in the gas phase.

Fig. 12a shows the calculated gas/aerosol partitioning of all product compounds, by mass, for the 888.5 $\mu g\,m^{-3}$ case. The calculated total condensed phase mass agrees closely with the measured value, and the mass of vapor phase products of 144 $\mu g\,m^{-3}$ is also very close to the 142.5 $\mu g\,m^{-3}$ predicted by Eq. (1). This degree of agreement is encouraging given that in the calculations the gas-phase product concentrations are derived essentially from the molar yields measured by Yu et al. (1999), giving the total quantities per m^3. By contrast in

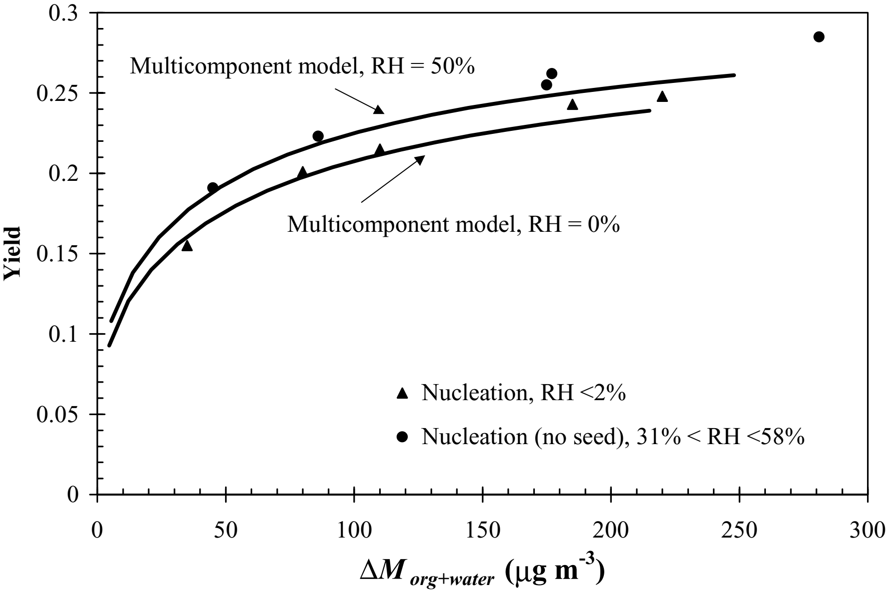

Fig. 11. Measured and calculated yields for systems without seed aerosol at 2% and 50% RH. Symbols—all data under these conditions. Solid line—multi-component model prediction.

the two-product model Eq. (1) the same information is obtained indirectly from the variation of ΔM_{org} with Δ(α-pinene). How consistent is the 12-product model with the two-product approach in Eq. (1), and can the products be assigned unambiguously to the two classes? Some 84.5% of the predicted gas-phase mass of 98.8 μg m^{-3} for Δ(α-pinene) = 888.5 μg m^{-3} is accounted for by compounds A9 and A10, of which only 5.7 μg m^{-3} occurs in the condensed phase. Also, 91% (193 μg m^{-3}) of the condensed phase is accounted for by compounds A2, A5, A6, A7, and A12, of which some 32 μg m^{-3} (mostly A5) is predicted to occur in the gas phase. The remaining products (A1, A3, A8, A13, and A14) are generated only in small amounts and contribute little to either phase. The only compound that occurs to a significant extent in both phases is A5. Adding this compound to A9 and A10 we obtain a total gas-phase organic concentration of 121.1 μg m^{-3}, which agrees closely with 121.8 μg m^{-3} predicted by Eq. (1).

We can also carry out a similar comparison for Δ(α-pinene) = 236.6 μg m^{-3}. Fig. 12b shows the calculated gas/aerosol partitioning of all product compounds, by mass, for the 236.6 μg m^{-3} case. For a condensed phase component, again consisting of A2, A5, A6, A7, and A12, a total aerosol amount of 34.6 μg m^{-3} is predicted by the present model, in essentially exact agreement with the 35 μg m^{-3} observed and the 33.65 μg m^{-3} obtained from Eq. (1). For this case, in which ΔM_{org} is smaller by a factor of > 6, the amount of the mainly condensed phase component that also exists in the gas phase is larger: 20.7 μg m^{-3} is predicted by Eq. (1), which is very close to the 22.7 μg m^{-3} obtained by the multi-product model. Most of this amount (14.1 μg m^{-3}) is contributed by compound A5. A total of 26.2 μg m^{-3} is contributed by compounds A9 and A10 to the gas phase, rising to 40.3 μg m^{-3} if A5 is included, agreeing closely with Eq. (1), which yields 38.6 μg m^{-3}. The amount of mainly gas-phase component occurring in the aerosol phase is only 1.35 μg m^{-3} from Eq. (1), which lies between the values predicted by the more complex model: 6.5 μg m^{-3} (A5 + A9 + A10) and 0.26 μg m^{-3} (A9 + A10 only).

In summary, comparison of the multi-product model with Eq. (1) for partitioning under dry conditions shows that for values of ΔM_{org} encompassing the measured range the two models agree closely in their predictions of gas-phase and particulate organic concentrations for aerosol systems. This suggests that the assumption underlying both models—equilibrium partitioning between a vapor phase and an aerosol phase in which the compounds are fully mixed—is correct. The result also implies that the molar yields of the product compounds obtained by Yu et al. (1999) are reasonable. This is because, if the total amounts used in the present model were significantly in error, then the model would not reproduce measured condensed phase amounts at the lower ΔM_{org} value, nor agree with the total masses of material predicted by Eq. (1) for both the examples examined above. The results of these calculations show that the primary condensed phase compounds are A2, A6, A7, and A12, and the gas-phase components are A9

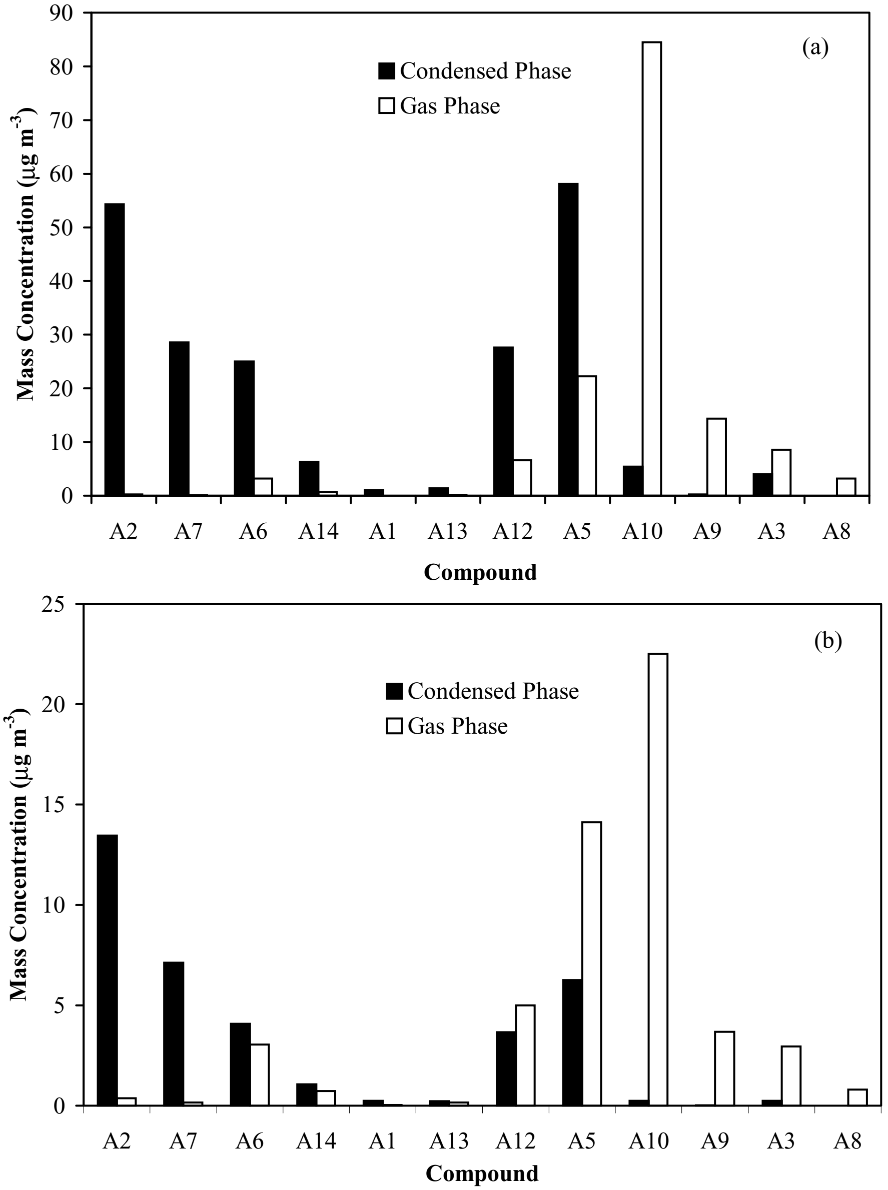

Fig. 12. Aerosol- and gas-phase concentrations of α-pinene oxidation products, for systems without salt seeds at 2% RH, calculated using the multi-product model described in Section 6.3.2. (a) Δ(α-pinene)= 888.5 μg m^{-3}; (b) Δ(α-pinene) = 225.5 μg m^{-3}. Refer to Table 5 for notation identifying each compound.

and A10. The partitioning of compound A5 varies with the total amount of material present and can exist in significant quantity in both phases.

Next, the multi-product model was applied to two experimental results including wet salt seed aerosol: 12/21a for $(NH_4)_2SO_4$ at 45.1% RH and Δ(α-pinene) = 365.5 μg m^{-3}, and 01/25b for $CaCl_2$ at 50% RH and Δ(α-pinene) = 623.7 μg m^{-3}. Calculations were carried out for both $\lambda_{\text{org, salt}} = 0$ and a range of positive values that correspond to a "salting out" effect. It was found that in all cases involving the $CaCl_2$ salt seed, and all except $\lambda_{\text{org, salt}} = 0$ for $(NH_4)_2SO_4$, the equilibrium system was predicted to contain an aerosol in which two liquid phases co-exist. The results of the calculations are summarized in Table 7. The predicted total aerosol volume of about 1.0×10^{-4} cm^3 m^{-3} for the $(NH_4)_2SO_4$ salt seed experiment is almost invariant with the value of the salting coefficient. The calculated total aerosol volume for the same conditions, but without the $(NH_4)_2SO_4$ seed, is 0.75×10^{-4} cm^3 m^{-3} and the volume

Table 7
Predicted phase partitioning

(a) System including $(NH_4)_2SO_4$ seed at 45.1% RH[a]

	Phase 1			Phase 2			
$\lambda_{\text{org, salt}}$	$\sum$ Org ($g\,m^{-3}$)	$n(NH_4)_2SO_4$ ($mol\,m^{-3}$)	nH_2O ($mol\,m^{-3}$)	$\sum$ Org ($g\,m^{-3}$)	$n(NH_4)_2SO_4$ ($mol\,m^{-3}$)	nH_2O ($mol\,m^{-3}$)	Volume ($(cm^3\,m^{-3})^b$)
0	8.3×10^{-5}	1.9×10^{-7}	5.8×10^{-7}	—	—	—	1.09×10^{-4}
0.01	7.8×10^{-8}	6.7×10^{-8}	1.9×10^{-7}	7.8×10^{-5}	1.3×10^{-7}	5.4×10^{-7}	1.06×10^{-4}
0.02	1.5×10^{-7}	1.6×10^{-7}	4.6×10^{-7}	7.5×10^{-5}	3.3×10^{-8}	3.1×10^{-7}	1.04×10^{-4}
0.05	5.4×10^{-8}	1.9×10^{-7}	5.5×10^{-7}	7.5×10^{-5}	2.5×10^{-11}	1.4×10^{-7}	1.03×10^{-4}
0.10	7.3×10^{-9}	1.9×10^{-7}	5.5×10^{-7}	7.5×10^{-5}	7.3×10^{-14}	1.4×10^{-7}	1.03×10^{-4}

(b) System including $CaCl_2$ seed at 50.0% RH[c]

$\lambda_{\text{org, salt}}$	$\sum$ Org ($g\,m^{-3}$)	$nCaCl_2$ ($mol\,m^{-3}$)	nH_2O ($mol\,m^{-3}$)	$\sum$ Org ($g\,m^{-3}$)	$nCaCl_2$ ($mol\,m^{-3}$)	nH_2O ($mol\,m^{-3}$)	Volume ($(cm^3\,m^{-3})^b$)
0	5.0×10^{-7}	1.1×10^{-7}	1.2×10^{-6}	1.6×10^{-4}	1.1×10^{-7}	1.2×10^{-6}	2.1×10^{-4}
0.01	5.4×10^{-7}	1.2×10^{-7}	1.3×10^{-6}	1.5×10^{-4}	1.0×10^{-7}	1.2×10^{-6}	2.1×10^{-4}
0.05	7.2×10^{-7}	1.6×10^{-7}	1.8×10^{-6}	1.5×10^{-4}	5.6×10^{-8}	9.3×10^{-7}	2.0×10^{-4}
0.10	6.1×10^{-7}	2.2×10^{-7}	2.4×10^{-6}	1.5×10^{-4}	1.1×10^{-11}	3.0×10^{-7}	2.0×10^{-4}
0.15	3.5×10^{-7}	2.2×10^{-7}	2.4×10^{-6}	1.5×10^{-4}	6.9×10^{-14}	3.0×10^{-7}	2.0×10^{-4}

[a] Conditions: experiment 12/21a, Δ(α-pinene) = 365.5 μg m^{-3}, $T = 301$ K, total $n(NH_4)_2SO_4 = 1.932\times10^{-7}$ mol.

[b] Total volume of both phases was calculated assuming that the apparent molar volumes of the salt and organic compounds are the same in mixed solutions as in pure (single solute) solutions.

[c] Conditions: experiment 01/25b, Δ(α-pinene) = 623.7 μg m^{-3}, $T = 301$ K, total $nCaCl_2 = 2.191\times10^{-7}$ mol.

of the aqueous salt seed alone is estimated to be $0.25\times10^{-4}\,cm^3\,m^{-3}$. Thus, subtracting the volume of the salt seed aerosol from the total to obtain $\Delta M_{\text{org+water}}$ yields almost exactly the value predicted for the system containing organic material and water alone. The same is true for the system containing aqueous $CaCl_2$ seed: here the total aerosol volume is calculated to be about $2.0\times10^{-4}\,cm^3\,m^{-3}$, and that of the salt seed alone $0.51\times10^{-4}\,cm^3\,m^{-3}$. The same system, but not including the salt seed, is calculated to have a total aerosol volume of $1.51\times10^{-4}\,cm^3\,m^{-3}$. Thus, again $\Delta M_{\text{org+water}}$ is predicted to be unaltered by the presence of the salt. The primary reason for this is that, for both cases, the liquid aerosol phase that contains the highest concentration (and largest amount) of organic material also contains only a very small fraction of the salt. The second liquid phase, by contrast, contains most of the salt but very little organic material. Consequently, the phase partitioning behavior differs little from that of salt/water and organic/water systems considered independently.

How realistic is the model? It has already been shown in Fig. 6 that the water activity/concentration relationship predicted by UNIFAC for the organic products of α-pinene oxidation is not consistent with the two growth factor measurements. This implies that the activities of the organic compounds are wrongly predicted to some degree. Also, the present calculations assume a liquid mixture in which the organic compounds are soluble. The model does not allow for the formation of solids—either salt or one or more organic compounds—with experiments including aqueous salt seed aerosols. If this were to occur then the apparent yield would be reduced. Furthermore, the pure compound vapor pressures of each of the organic oxidation products are only estimates, and little is known about the interaction of complex multi-functional organic products with salts, which are parameterized here in a very simple way.

While this model does not reproduce the reduced yields for the aqueous salt seed cases found in the experiments, the errors are less than for the two component, single liquid phase, model discussed in the previous section. In those calculations the predicted yields were increased relative to the no seed case, particularly for low $\Delta M_{\text{org+water}}$, due to the organic products partitioning into the water associated with the salt aerosol. In the two liquid phase case this effect is largely absent. Consequently, it seems reasonable that the predicted yield could be reduced relative to the no seed case for some sets of thermodynamic properties of the organic compounds, and that two liquid phases may be forming in the aerosols. However, this is yet to be proven.

7. Aerosol-phase reactions

The presence of aqueous salt seed aerosols affects the partitioning of the organic products of α-pinene oxidation, but it has not been possible to model the results based on a simple "salting out" effect. In our calculations we have assumed that all oxidation occurs in the gas phase, followed by gas–particle partitioning into the aerosol phase. However, there is some experimental evidence of aerosol phase chemistry occurring in similar systems. Tobias and Ziemann (2000) have recently reported the identification of such products in the ozonolysis of 1-tetradecene using a thermal desorption mass spectrometer. These hemiacetals and acetals readily hydrolyze and would not be detected using conventional sampling techniques such as those employed by Yu et al. (1999) for identifying the products of the α-pinene/O_3 reaction. The presence of electrolytes in the organic aerosol may affect the rate or inhibit such reactions. A reduction in the formation of these less volatile organic compounds would cause a reduction in the aerosol yield.

8. Summary and conclusions

An extensive investigation into the aerosol forming potential of α-pinene/O_3 oxidation under dry and humid conditions has been carried out. It was found, first, that in a system containing only organic compounds and water the total aerosol yield at 50% RH was increased relative to that under dry conditions due to the uptake of water. Second, the presence of a dry inorganic salt aerosol in the system had no measurable effect on the aerosol yield of organic material. Third, in experiments where there was a pre-existing aqueous salt seed aerosol then the yield of organic material plus associated water was reduced relative to the no seed (or dry seed) cases over the full range of amounts of α-pinene reacted. The effect differs according to the salt, with $(NH_4)_2SO_4$ causing the greatest reduction in yield per mole of salt present, and $CaCl_2$ the smallest reduction.

Growth factors for the condensed organic material were determined at 50% and 85% RH and used to estimate possible activity/concentration relationships according to the assumption of both a fully liquid aerosol, and one in which only about 50% of the organic material dissolves (the rest existing as a solid or other separate phase). Measurements of the aerosol yield at the higher relative humidities (RH), in experiments without salt seeds, were better predicted by the two component mole fraction based model on the assumption of 50% solubility of the organic material in the aerosol phase. However, as the growth factors were determined at only two RHs, and the solubility of the organic material in water is not known, no certain conclusions can be drawn from these calculations. It is also possible to reproduce the aerosol yields using an activity coefficient model in which both the water and organic components are greater than unity in the mixture, though this behavior appears not to be consistent with the growth factor data.

The aerosol yield was also modeled, using the two-component model, for cases in which an aqueous salt seed aerosol was present. In these cases a single liquid aerosol phase was assumed and various organic/salt interactions ("salting in" and "salting out") were tried, parameterized in a simple thermodynamically consistent set of equations. In all cases it was found that the predicted yield of organic material was increased relative to the no-seed case, mainly due to the larger volume of water available for the organic material to dissolve into. This predicted increase in yield is particularly large at small values of $\Delta M_{\mathrm{org+water}}$. Even high degrees of salting out did not greatly affect the predicted total yield of organic material and water. It is noted that a positive salting coefficient, which corresponds to salting out of the organic material from the particle phase, also increases the osmotic coefficient and thus the water uptake by an aerosol containing significant concentrations of both salt and dissolved organic matter at a fixed RH. The possible effect of partial solubility of the condensed organic material—presumably producing a largely organic phase in the aerosol in addition to the aqueous (salt containing) component—was not investigated. However, it appears most likely that such behavior would produce a yield similar to, but not less than, a system containing no salt seed. The possibility that the partitioning of the organic material to the aerosol phase causes the crystallization of the salt seed would reduce the apparent yield. However, this could only occur for the $(NH_4)_2SO_4$ seed, whose deliquescence RH is about 80%.

The two-component model of partitioning was compared with a more realistic one which included the twelve major product compounds identified by Yu et al. (1999) and pure compound vapor pressures estimated using semi-empirical methods. The compounds making up the "more condensable" and "less condensable" components in the simpler model were identified, and very close agreement was found between the two approaches for calculations under dry conditions.

Laboratory experiments on aqueous solutions containing dissolved pinic acid, which is thought to be a major condensable product of α-pinene, showed that two liquid phases form in the presence of the salt $(NH_4)_2SO_4$. Model calculations in which activity coefficients of the soluble organic compounds were calculated by UNIFAC for organic/water interactions in Eqs. (10) and (12) also predicted an aerosol containing two liquid phases, though we note that water activity coefficients in solutions containing the organic products calculated by UNIFAC are not consistent with measured growth factors. Calculated aerosol yields for the 12-product model for the experiments with aqueous salt seeds, although too high, were closer to the measured values than was the case with the simpler model. This suggests that an aerosol containing two distinct phases may explain the reduced yields that are observed.

All the calculations presented here assume that the oxidation of α-pinene occurs in the gas phase and that the products, which do not themselves further react, partition between the aerosol and vapor phases. Other work, referred to above, suggests that further reactions may occur in the condensed phase probably to form products of lower vapor pressure than the reactants. These reactions, which might be affected either positively or negatively by the presence of salts, would tend to increase the yield with time.

It has not been possible to match the reduction in aerosol yield caused by the presence of aqueous salt seed using the models presented here, and a better understanding of what is occurring in the aerosol phase is needed. Further experiments should determine, first, the solubility in water of compounds most likely to partition significantly into the aerosol phase, and also the activity/concentration relationships of the aqueous solutions. Second, the effect of salts on aqueous solutions of the organic products should be investigated, including both the formation of multiple phases and the influence of the salt on the water and organic compound activities. A better knowledge of other fundamental properties, such as the vapor pressures of the principal products of α-pinene oxidation, would be valuable.

Acknowledgements

This work was supported by the US Environmental Protection Agency Center on Airborne Organics, US Environmental Protection Agency Agreement CR827331-01-0, and the Chevron Corporation. David Cocker was supported in part by a NSF Graduate Fellowship. The contribution of Simon Clegg was supported by an Advanced Fellowship from the Natural Environment Research Council of the UK. Special thanks to K.M. Cocker, M. Kalberer, and N.E. Whitlock.

References

Anathaswamy, J., Atkinson, G., 1985. Thermodynamics of concentrated electrolyte mixtures. 5. A review of the thermodynamic properties of aqueous calcium chloride in the temperature range 273.15–373.15 K. Journal of Chemical and Engineering Data 30, 120–128.

Ansari, A.A., Pandis, S.N., 2000. Water absorption by secondary organic aerosol and its effect on inorganic aerosol behavior. Environmental Science and Technology 34, 71–77.

Bilde, M., Pandis, S.N., 2000. Evaporation rates of α pinene photooxidation aerosol products. Journal of Aerosol Science 31 (Suppl. 1), S174–S175.

Clegg, S.L., Pitzer, K.S., Brimblecombe, P., 1992. Thermodynamics of multicomponent, miscible, ionic solutions. II. Mixture including unsymmetrical elctrolytes. Journal of Physical Chemistry 96, 9470–9479.

Clegg, S.L., Ho, S.S., Chan, C.K., Brimblecombe, P., 1995. Thermodynamic properties of aqueous $(NH_4)_2SO_4$ to high supersaturation as a function of temperature. Journal of Chemical and Engineering Data 40, 1079–1090.

Clegg, S.L., Brimblecombe, P., Wexler, A.S., 1998a. A thermodynamic model of the system H^+–NH_4^+–Na^+–SO_4^{2-}–NO_3^-–Cl^-–H_2O at 298.15 k. Journal of Physical Chemistry 102, 2155–2171.

Clegg, S.L., Brimblecombe, P., Wexler, A.S., 1998b. A thermodynamic model of the system H^+–NH_4^+–SO_4^{2-}–NO_3^-–H_2O at tropospheric temperatures. Journal of Physical Chemistry 102, 2137–2154.

Clegg, S.L., Seinfeld, J.H., Brimblecombe, P., 2001. Thermodynamic modeling of aqueous aerosols containing electrolytes and dissolved organic compounds. Journal of Aerosol Science 32, 713–738.

Cocker, D.R., Fiagan, R.C., Seinfeld, J.H., 2001a. State-of-the-art chamber facility for studying atmospheric aerosol chemistry. Environmental Science and Technology 35, 2594–2601.

Cocker, D.R., Whitlock, N.W., Flagan, R.C., Seinfeld, J.H., 2001b. Hygroscopic properties of Pasadena, California, aerosol. Aerosol Science and Technology 35, 637–647.

Collins, D.R., Flagan, R.C., Seinfeld, J.H., 2001. Improved inversion of scanning DMA data. Aerosol Science and Technology, in press.

Cruz, N.C., Pandis, S.N., 2000. Deliquescence and hygroscopic growth of mixed inorganic–organic atmospheric aerosol. Aerosol Science and Technology 34, 4313–4319.

Edney, E.O., Driscoll, D.J., Speer, R.E., Weathers, W.S., Kleindienst, T.E., Li, W., Smith, D.F., 2000. Impact of aerosol liquid water on secondary organic aerosol yields of irradiated toluene/propylene/NO_x/$(NH_4)SO_4$/air mixtures. Atmospheric Environment 34, 3907–3919.

Ferron, G.A., Karg, E., Busch, B., Heyder, J., 1999. Hygroscopicity of ambient particles. Journal of Aerosol Science 30, S19–S20.

Forstner, H.J.L., Flagan, R.C., Seinfeld, J.H., 1997. Secondary organic aerosol from the photooxiation of aromatic hydrocarbons: molecular composition. Environmental Science and Technology 31, 1345–1358.

Fredenslund, Aa., Jones, R.L., Prausnitz, J.M., 1975. Group-contribution estimation of activity coefficients in non-ideal liquid mixtures. AIChE Journal 21, 1086–1098.

Griffin, R.J., Cocker III, D.R., Flagan, R.C., Seinfeld, J.H., 1999. Organic aerosol formation from the oxidation of biogenic hydrocarbons. Journal of Geophysical Research 104, 3555–3567.

Hansen, H.K., Rasmussen, P., Fredenslund, A., Schiller, M., Gmehling, J., 1991. Vapor–liquid equilibria by UNIFAC group contribution. 5. Revision and extension. Industrial and Engineering Chemistry Research 30, 2352–2355.

Hoffmann, T.P.W., Odum, J.R., Bowman, F., Collins, D.R., Klockow, D., Flagan, R.C., Seinfeld, J.H., 1997. Formation of organic aerosols from the oxidation of biogenic hydrocarbons. Journal of Atmospheric Chemistry 26, 189–222.

Jacobson, M.Z., Tabazadeh, A., Turco, R.P., 1996. Simulating equilibrium within aerosols and nonequilibrium between gases and aerosols. Journal of Geophysical Research 101, 9079–9091.

Kim, Y.P., Seinfeld, J.H., 1995. Atmospheric gas–aerosol equilibrium, III, thermodynamics of crustal elements CA^{2+}, K^+, and Mg^{2+}. Aerosol Science and Technology 22, 93–110.

Kim, Y.P., Seinfeld, J.H., Saxena, P., 1993a. Atmospheric gas–aerosol equilibrium, I, thermodynamic model. Aerosol Science and Technology 19, 157–181.

Kim, Y.P., Seinfeld, J.H., Saxena, P., 1993b. Atmospheric gas–aerosol equilibrium, II, analysis of common approximations and activity coefficient calculation methods. Aerosol Science and Technology 19, 182–198.

Massling, A., Wiedensohler, A., Busch, B., 1999. Hygroscopic growth of aerosol particles in the Southern Atlantic Ocean and Indian Ocean. Journal of Aerosol Science 30, S837–S838.

McMurry, P.H., Stolzenburg, M.R., 1989. On the sensitivity of particle size to relative humidity for Los Angeles aerosols. Atmospheric Environment 23, 497–507.

Myrdal, P.B., Yalkowsky, S.H., 1997. Estimating pure component vapor pressures of complex organic molecules. Industrial and Engineering Chemistry Research 36, 2494–2499.

Nenes, A., Pandis, S.N., Pilinis, C., 1998. ISORROPIA: A new thermodynamic equilibrium model for multiphase multicomponent inorganic aerosols. Aqua Geochemistry 4, 123–152.

Odum, J.R., Hoffmann, T.P.W., Bowman, F., Collins, D., Flagan, R.C., Seinfeld, J.H., 1996. Gas/particle partitioning and secondary organic aerosol yields. Environmental Science and Technology 30, 2580–2585.

Odum, J.R., Jungkamp, T.P.W., Griffin, R.J., Forstner, H.J.L., Flagan, R.C., Seinfeld, J.H., 1997. Gas/particle partitioning of semivolatile organic compounds to model inorganic, organic, and ambient smog aerosols. Science 276, 96–99.

Pankow, J.F., 1994a. An absorption-model of gas–particle partitioning of organic-compounds in the atmosphere. Atmospheric Environment 2, 185–188.

Pankow, J.F., 1994b. An absorption-model of the gas aerosol partitioning involved in the formation of secondary organic aerosol. Atmospheric Environment 2, 189–193.

Pilinis, C., Seinfeld, J.H., 1987. Continued development of a general equilibrium model for inorganic multicomponent atmospheric aerosols. Atmospheric Environment 32, 2453–2466.

Rader, D.J., McMurry, P.H., 1986. Application of the tandem differential mobility analyzer to studies of droplet growth or evaporation. Journal of Aerosol Science 17, 771–787.

Robinson, R.A., Stokes, R.H., 1959. Electrolyte Solutions: the Measurement and Interpretation of Conductance, Chemical Potential, and Diffusion in Solutions of Simple Electrolytes, 2nd edition. Academic Press, New York.

Saxena, P., Hildemann, L.M., 1997. Water absorption by organics: survey of laboratory evidence and evaluation of UNIFAC for estimating water activity. Environmental Science and Technology 31, 3318–3324.

Sohnel, O., Novotny, P., 1985. Densities of Aqueous Solutions of Inorganic Substances. Elsevier, Amsterdam.

Svenningsson, I.B., Hansson, H.C., Wiedensohler, A., Ogren, J.A., Noone, K.J., Hallberg, A., 1992. Hygroscopic growth of aerosol particles in the Po Valley. Tellus. 44B, 556–569.

Swietlicki, E., Zhou, J., Berg, O.H., Martinsson, B.G., Frank, G., Cederfelt, S.-I., Dusek, U., Berner, A., Birmili, W., Wiedensohler, A., Yuskiewicz, B., Bower, K.N., 1999. A closure study of sub-micrometer aerosol particle hygroscopic behaviour. Atmospheric Research 50, 205–240.

Tang, I.N., Munkelwitz, H.R., 1994. Water activities, densities, and refractive-indexes of aqueous sulfates and sodium-nitrate droplets of atmospheric importance. Journal of Geophysical Research—Atmosphere 99, 18801–18808.

Tobias, H.J, Ziemann, P.J., 2000. Thermal desorption mass spectrometric analysis of organic aerosol form from reactions of 1-tetradecene and O_3 in the presence of alcohols and carboxylic acids. Environmental Science and Technology 34, 2105–2115.

Virkkula, A., Dingenen, R.V., Raes, F., Hjorth, J., 1999. Hygroscopic properties of aerosol formed by oxidation of limonene, α-pinene, and β-pinene. Journal of Geophysical Research 104, 3569–3579.

Wexler, A.S., Clegg, S.L., 2001. Atmospheric aerosol models for systems including the ions H^+, NH_4^+, Na^+, SO_4^{2-}, NO_3^-, Cl^-, Br^- and H_2O. Journal of Geophysical Research, submitted

Wexler, A.S., Seinfeld, J.H., 1990. The distribution of ammonium salts among a size and composition dispersed aerosol. Atmospheric Environment 24A, 1231–1246.

Wexler, A.S., Seinfeld, J.H., 1991. Second-generation inorganic aerosol model. Atmospheric Environment 25A, 2731–2748.

Yu, J., Cocker III, D.R., Griffin, R.J., Flagan, R.C., Seinfeld, J.H., 1999. Gas-phase oxidation of monoterpenes: gaseous and particulate products. Journal of Atmospheric Chemistry 34, 207–258.

Zhang, Y., Seignoir, C., Seinfeld, J.H., Jacobson, M., Clegg, S.L., Binkowski, F.S., 2000. A comparative review of inorganic aerosol thermodynamic equilibrium modules: similarities, differences, and their likely causes. Atmospheric Environment 34, 113–117.